

# Comprehensive Automobile Research System (CARS) – a

## Python-based Automobile Emissions Inventory Model

Bok H. Baek<sup>1</sup>, Rizzieri Pedruzzi<sup>2</sup>, Minwoo Park<sup>3</sup>, Chi-Tsan Wang<sup>1</sup>, Younha Kim<sup>3</sup>, Chul-Han Song<sup>4</sup>, and Jung-Hun Woo<sup>3</sup>

<sup>1</sup>Center for Spatial Information Science and Systems – George Mason University, Fairfax, VA, USA.

<sup>2</sup>Department of Sanitary and Environmental Engineering, Federal University of Minas Gerais, Belo Horizonte, Brazil.

<sup>3</sup>Department of Advanced Technology Fusion, Konkuk University, Republic of Korea

<sup>4</sup>School of Earth and Environmental Engineering, Gwangju Institute Science and Technology, Republic of Korea

*corresponding to: Jung-Hun Woo (jwoo@konkuk.ac.kr)*

### Abstract

The Comprehensive Automobile Research System (CARS) is an open-source python-based automobile emissions inventory model designed to efficiently estimate high quality emissions from motor-vehicle emission sources. It can estimate the criteria air pollutants, greenhouse gases, and air toxics in various temporal resolutions at the national, state, county, and any spatial resolution based on the spatiotemporal resolutions of input datasets. The CARS is designed to utilize the local **vehicle activity data**, such as vehicle travel distance, road link-level network Geographic Information System (GIS) information, and vehicle-specific average speed by road type, to generate a temporally and spatially **resolved** automobile emissions inventory for policymakers, stakeholders, and the air quality modeling community. The CARS model adopted the European Environment Agency's (EEA) onroad automobile emissions calculation methodologies to estimate the hot exhaust, cold start, and evaporative emissions from onroad automobile sources. **It can optionally utilize average speed distribution (ASD) of all road types to reflect more realistic vehicle speed variations.** Also, utilizing high-resolution road GIS data allows the CARS to estimate the road link-level emissions to improve the inventory's spatial resolution. When we compared the official 2015 national mobile emissions from Korea's Clean Air Policy Support System (CAPSS) against the ones estimated by the CARS, there is a moderate increase of volatile organic compounds (VOCs) (33%), carbon monoxide (CO) (52%), and fine particulate matter (PM<sub>2.5</sub>) (15%) emissions while nitrogen oxides (NO<sub>x</sub>) and sulfur oxides (SO<sub>x</sub>) are reduced by 24% and 17% in the CARS estimates. The main differences are driven by the usage of different vehicle activities and the incorporation of road-specific ASD, which plays a critical role in hot

exhaust emission estimates but wasn't implemented in Korea's CAPSS mobile emissions inventory. While 52% of vehicles use gasoline fuel and 35% use diesel, gasoline vehicles only contribute 7.7% of total NO<sub>x</sub> emissions while diesel vehicles contribute 85.3%. But for VOC emissions, gasoline vehicles contribute 52.1% while diesel vehicles are limited to 23%. While diesel buses are only 0.3% of vehicles, each vehicle has the largest contribution to NO<sub>x</sub> emissions (8.51% of NO<sub>x</sub> total) due to it having longest daily vehicle kilometer travel (VKT). In VOC emission part, CNG buses are the largest contributor with 19.5% of total VOC emissions. For primary PM<sub>2.5</sub>, more than 98.5% is from diesel vehicles. The CARS model's in-depth analysis feature can assist government policymakers and stakeholders develop the best emission abatement strategies.

Keywords: inventory: automobile, vehicle emissions, hot exhaust, cold start, evaporative, python

## 1 Introduction

Globally, ambient pollution causes more than 4.2 million premature deaths every year (Cohen et al., 2017), and Burnett et al. estimate the health burden is closer to 9 million deaths from ambient PM concentrations (Burnett et al., 2018). To effectively mitigate air pollutants, both developed and developing countries' governments have been implementing stringent air pollution abatement control policies to reduce harmful regional air pollutants (Hogrefe et al., 2001a; Hogrefe et al., 2001b; Dennis et al., 2010; Rao et al., 2011; Appel et al., 2013; Luo et al., 2019). The CTM simulation results strongly rely on precise input data, such as emission inventory, meteorology, land surface parameters, and chemical mechanisms in the atmosphere.

The transportation emission sector is one of the major anthropogenic emissions in urban areas. The tailpipe emissions from the vehicle's combustion process contain many air pollutants, including nitrogen oxides (NO<sub>x</sub>), volatile organic compounds (VOCs), carbon monoxide (CO), ammonia (NH<sub>3</sub>), sulfur dioxide (SO<sub>2</sub>), and primary particulate matter (PM) which will participate in the formation of detrimental secondary pollutants like ozone and PM<sub>2.5</sub> in the atmosphere. In the Seoul Metropolitan Area (SMA) in South Korea, transportation automobile sources contribute the most to the total NO<sub>x</sub> and primary PM<sub>2.5</sub> emissions across all emission sources. (Choi et al., 2014; Kim et al., 2017a; Kim et al., 2017b; Kim et al., 2017c). Thus, it is critical to understand and represent better on the emission patterns from the transportation automobile sources in the CTM model. The use of process-based automobile emission models is highly recommended to meet the needs in CTM model because it can estimate the highly resolved spatiotemporal automobile emissions. (Moussiopoulos et al., 2009; Russell and Dennis, 2000).

There are two methodologies known in emission inventory development: top-down and bottom-up. The choice of methods is determined by the input data availability. The top-down approach primarily relies on the aggregated and generalized country or regional information,

68 especially in developing countries where only limited datasets and information are available. It has  
69 its limitations on representing the vehicle emission process realistically due to the lack of detailed  
70 activity and ancillary supporting data. However, the bottom-up approach requires higher-quality  
71 spatiotemporal activity datasets like road network information, vehicle composition (vehicle type,  
72 engine size, vehicle age, and fuel-technology), pollutant-specific emissions factors, road segment  
73 length, traffic activity data, and fuel consumption (EEA, 2019; Ibarra-Espinosa et al., 2018b;  
74 IEEMA, 2017). It can generate more accurate and detailed automobile emissions across various  
75 operating processes, such as hot exhaust, evaporative, idling, and hot soak (Nagpure et al., 2016;  
76 Ibarra-Espinosa et al., 2018a).

77 There are several bottom-up mobile emissions models available, like MOVES (MOtor  
78 Vehicle Emissions Simulator) from the U.S. Environmental Protection Agency (USEPA), the  
79 European Environment Agency's (EEA) model COPERT (COmputer Programmed to calculate  
80 Emissions from Road Transport), the HERMES (High-Elective Resolution Modelling Emission  
81 System) from Barcelona Supercomputing Center (Guevara et al., 2019), the VEIN (Vehicular  
82 Emissions INventory) model developed by Ibarra-Espinosa et al. (2017), and the VAPI (Vehicular  
83 Air Pollution Inventory) model developed by Nagpure and Gurjar (2012) for India (Nagpure et al.,  
84 2016). While these models are all bottom-up emission inventory models, a single model cannot  
85 meet all modelers, policymakers, and stakeholders' needs because each model holds its own pros  
86 and cons. They are developed differently to meet specific user needs based on the types of traffic  
87 activity and emission factors, emission calculation methodologies, and other optional/available  
88 traffic-related inputs such as average speed distribution and geographical resolution. Each model  
89 is developed with different levels of specificity, underlying data set and modeling assumptions.

90 The MOVES model has the strength to generate high-quality emissions for up to 16  
91 different emission processes (i.e., Running Exhaust, Start Exhaust, Evaporative, Refueling,  
92 Extended Idling, Brake, Tire, etc.). It can simulate not only county-level but also road segment  
93 level depending on data availability. It can also reflect local meteorological conditions, such as  
94 ambient temperature and relative humidity, which can significantly impact both pollutants and  
95 emissions processes (Choi et al., 2017; Perugu et al., 2018). Disadvantage of this model is it  
96 difficult to update and apply to countries outside of the U.S. because MOVES model is high degree  
97 of specificity. The COPERT model that is widely used in European countries has its advantages,  
98 such as the capability to model emissions in high resolution. Additionally, it is fully integrated  
99 with the EEA's onroad vehicle emissions factors guidelines and can generate a complete quality  
100 assurance (QA) and visualization summary (Ntziachristos et al., 2009). The cons are that it is a  
101 proprietary commercial licensed software, limited to EEA guidance, and challenging to modify  
102 and update with any key input datasets like the latest emission factors from non-European  
103 countries (Lejri et al., 2018; Rey DR, 2021; Li et al., 2019; Lv et al., 2019; Smit et al., 2019).

104 The HERMES and VEIN are both recently released bottom-up inventory models. They  
105 have their pros in that they are both open-source models based on open-source computing

languages (Python and R), which provide transparency of emission calculations with a considerable amount of data behind it (Ibarra-Espinosa et al., 2018b; Guevara et al., 2019). Both models are driven by comma-separated value (CSV) formatted input files, making it very easy for users to modify the input datasets. They are also based on the EEA's emission calculation method and equipped with a complete QA and visualization tool based on Python and R libraries. However, it is not an easy task to update the emission factors, and generate other required input datasets for other countries, and lacks support for any control strategy plan feature to generate a responsive reduced emissions inventory for policymakers, stakeholders, and modelers.

The VAPI (Vehicular Air Pollution Inventory) model was developed in India because the country does not have an extensive and robust traffic-related dataset to run these kinds of vehicular emissions inventory models (Nagpure et al., 2016; Perugu, 2019).

There are also a few shortcomings of incorporating these bottom-up models into CTM studies. These models require strong programming skills to operate, such as collecting and preparing the input data to fit the model requirement, configuring the model variables, and changing specific variables that may be embedded in the code. Another downside is that while the administration-level emissions inventory can be estimated by those models, it requires a 3<sup>rd</sup> party emissions processor like the SMOKE (Sparse Matrix Operator Kerner Emissions) modeling system (Baek and Seppanen, 2021) to process and generate spatially and temporally resolved emissions inputs for CTM. Some detailed information, like link-level hourly driving patterns, can be lost in the emissions processing steps.

There is no single model capable of meeting all the requirements across various spatial and temporal scales (Pinto et al., 2020). However, transparency, simplicity, and a user-friendly interface are requirements for those who mainly work in transportation policy and air quality modeling development (Fallahshorshani et al., 2012; Kaewunruen et al., 2016; Sallis et al., 2016; Sun et al., 2016; Tominaga and Stathopoulos, 2016). Thus, the ideal mobile emissions modeling system would be computationally optimized, easy-to-use, and have a user-friendly interface. Additionally, the model should easily adapt detailed local activity information and the state-of-art emission factors as an input to represent them in the highest resolution possible in time and space.

We have developed the Comprehensive Automobile Research System (CARS) to meet these requirements, especially for the air quality research community, policymakers, and air quality modelers. The CARS is a stand-alone, fully modularized, computationally optimized, python-based automobile emission model. The modularization improves the efficiency of processing times. Once district and road link-level annual/monthly/daily total emissions are computed, the rest of the processes are optional. It can generate chemically speciated, spatially gridded hourly emissions for CTMs without any 3<sup>rd</sup> party emissions modeling system to develop the highest quality CTM-ready emissions inputs. All functions are operated by independent modules and can be enabled by users. Details on modularization will be discussed later. The CARS model can be easily adopted

and is simple for users to add new functions or modules in the future. The application of the CARS to South Korea will be described in detail later.

## 2 CARS Emissions Calculation

The CARS is an open-source Python-based customizable motor vehicle emissions processor that estimates onroad and offroad emissions for specific criteria and toxic air pollutants. Figure 1 is a schematic of the CARS overview. It applies vehicle, engine, and fuel specific emission factors to traffic data to estimate the local level annual, monthly, and daily total emissions inventory. The emissions inventory calculations require the list of pollutant-specific emissions factors by vehicle age, local activity data, average speed profile/distribution by road type, and geographic information system (GIS) road segment shapefiles inputs. The spatial resolution of vehicle kilometer travel (VKT) defines the CARS geographic scale (i.e. district, county, state, and country) for emission calculations. Unlike the district-level Korea Clean Air Policy Support System (CAPSS) automobile emission inventory (Lee et al., 2011a; Lee et al., 2011b), the CARS applies high-resolution annual average daily traffic (AADT) data from the road GIS shapefiles to distribute the total district emissions into road link-level emissions. Optionally, these road link-level emissions can be used to generate spatially gridded CTM-ready emissions input data once the output modeling domain is defined. The summary of input files by categories are presented in Appendix H. How the CARS estimates spatially and temporally enhanced automobile emissions inventories will be discussed in detail next chapter.

South Korean traffic databases from the Korea CAPSS team (Lee et al., 2011b) from the National Institute of Environmental Research (NIER) were used in this study to compute the updated onroad automobile emissions inventory. The databases include individual vehicle activity data (daily total VKT), road activity data (average speed distribution by road), vehicle age specific emission factors, road type information, surface weather data, and GIS road shapefiles.

### 2.1 Individual Daily Average VKT Activity Data

The individual vehicle VKT data is used to reflect the human activity. This study imported the national registered vehicle-specific daily total VKT from South Korea's Vehicle Inspection Management System (VIMS), which belongs to the Korea Transportation Safety Authority (KTSA). It contains over 50 million records from 2013 to 2017. For the CARS model, we first sorted these records by the vehicle identification number (VIN) to remove any duplicates and then built vehicle-specific daily total VKT traffic activity data in the CSV format. The summary of those vehicle numbers and VKTs is presented in Fig. 2. Sedan vehicles using gasoline fuel comprise the greatest percentage of total vehicles at 47% (~10.4 million) and have the highest VKT. Most vehicles demonstrate similar patterns between the number of vehicles and daily VKT.

However, as expected, LPG (liquefied petroleum gas)-fueled taxi are high in VKT compared to the number of vehicles due to their daily long distance travel pattern.

The VIN ( $vin$ ) information is used to calculate vehicle-specific daily average VKT ( $VKT_{vin}$ , km d<sup>-1</sup>). In Eq. (1), the individual daily average vehicle VKT ( $VKT_{vin}$ ) is calculated based on the cumulative mileage ( $M_{f;vin}$ ) between the last inspection date ( $D_{f;vin}$ ) and registration date ( $D_{0;vin}$ ). Each vehicle is categorized with Korea's NIER defines the vehicle types (Ryu et al., 2003; Ryu et al., 2004; Ryu et al., 2005; Lee et al., 2011a) that based on a combination of vehicle types (e.g., sedan, truck, bus, etc), engine sizes (e.g., compact, full size, midsize, etc) and fuel types (e.g., gasoline, diesel, LPG, etc). Full details of vehicle types and daily total VKT are shown in Appendix A and B.

$$VKT_{vin} = \frac{M_{f;vin}}{D_{f;vin} - D_{0;vin}} \quad (1)$$

## 2.2 Emission Calculations

Automobile emission sources include motorized engine sources on the paved road network including off-network (e.g., drive way and parking lots). The CARS model doesn't simulate emissions from nonroad emission sources, such as aviation, railways, construction, agricultures, lawn mower, and boats yet. The CARS model simulates the onroad automobile emissions from network roads using their local traffic-related datasets. The following section explains the approach of the onroad automobile emission processes. The onroad emission ( $E_{onroad}$ ) in the CARS is defined in Eq. (2), which includes three major emission processes (Ntziachristos and Samaras, 2000):

$$E_{onroad} = E_{hot} + E_{cold} + E_{vap} \quad (2)$$

The hot exhaust emissions ( $E_{hot}$ ) are the vehicle's tailpipe emissions when the internal combustion engine (ICE) combusts the fuel to generate energy under the average operating temperature. The cold start emissions ( $E_{cold}$ ) are the tailpipe emissions from the ICE when the cold vehicle engine is ignited and the operational temperature is below average condition. The evaporative VOC emissions ( $E_{vap}$ ) are the emissions evaporated/permeated from the fuel systems (fuel tanks, injection systems, and fuel lines) of vehicles.

The CARS first applies the hot exhaust emission factors by vehicle type, age, fuel, engine, and pollutants to individual daily total VKT to compute the hot exhaust emissions. The rest of the processes for cold start and evaporative emissions are calculated afterwards. The emission calculation methodologies used in the CARS model are based on tier 2 and tier 3 methodologies from the EEA's mobile emission inventory guidebook (EEA, 2019) to be consistent with Korea's National Emission Inventory System (NEIS) (Lee et al., 2011a).



### 2.2.1 Hot Exhaust Emissions

Hot exhaust emissions, which is from the vehicle's tailpipe, is the exhaust gas from the combustion process in an ICE. The ICE combustion cycle generally causes incomplete combustion processes which emit hydrocarbons, carbon monoxide (CO), and particulate matter (PM) which not completely controlled from the aftertreatment equipment, such as three-way catalytic converter and released into the atmosphere. The sulfur compounds in the fuel are oxidized and become sulfur oxides (SO<sub>x</sub>). Nitrogen oxides (NO<sub>x</sub>) are produced during the combustion process due to the abundant nitrogen (N<sub>2</sub>) and oxygen (O<sub>2</sub>) in the atmosphere.

Equation 3 represents the calculation of daily individual vehicle hot exhaust emission rate,  $E_{hot; p, vin, myr}$  (g d<sup>-1</sup>) of pollutant ( $p$ ). An individual vehicle-specific daily  $VKT_{vin}$  (km d<sup>-1</sup>) is estimated by Eq. (1). The  $EF_{hot; p, v, myr, s}$  (g/km) is the hot exhaust emission factor of pollutants ( $p$ ) for the vehicle type ( $v$ ), vehicle manufacture year ( $myr$ ), and average vehicle speed ( $s$ ). The district's total emission rate is the total hot exhaust emissions from all individual vehicles within the same district.

$$E_{hot; p, vin, myr} = DF_{p, v, myr} \times VKT_{vin} \times EF_{hot; p, v, myr, s} \quad (3)$$

The deterioration factor ( $DF$ ) in Eq. (3) is an optional function in the CARS. The deterioration process is caused by vehicle aging and can lead to the increase of vehicle emissions. The vehicle  $DF$  is varied by vehicle type ( $v$ ), pollutant ( $p$ ), and vehicle manufacture year ( $myr$ ). The CARS model computes vehicle ages based on the vehicle manufacture year and model simulation year. According to the guidance of deterioration factors calculation from NIER, there is no deterioration in a new vehicle during their first five years. After five years, the deterioration factors can increase the 5~10% range depending on the type of vehicle and pollutants. Deterioration processes can cause up to 100% increase of emissions in fifteen-year-old vehicles. Currently, the  $DF$  is an empirical coefficient that varies by vehicle age (Lee et al., 2011a).

The hot exhaust emission factor,  $EF_{hot; p, v, s}$  (g/km) is a function of vehicle speed ( $s$ ) with other empirical coefficients:  $a, b, c, d, f, k$ . The emission factor formula and those coefficients were developed by NIER CAPSS (Lee et al., 2011a). These coefficients are varied by pollutants ( $p$ ), vehicle type ( $v$ ), vehicle manufacture year ( $myr$ ), and vehicle speed ( $s$ ). The vehicle speed affects the combustion efficiency of an ICE and impacts the emission rates and its composition from the tailpipe.

$$EF_{hot; p, v, myr, s} = k(a \times s^b + c \times s^d + f) \quad (4)$$

While vehicle speed plays a critical role in hot exhaust emissions from most vehicles, NO<sub>x</sub> emissions from some diesel vehicles show sensitivity to local ambient temperature along with vehicle speed (Ntziachristos and Samaras, 2000). Figure 3 shows the dependency of NO<sub>x</sub> emission factors from compact diesel vehicles to vehicle speed (Fig. 3a) and ambient temperature (Fig. 3b).

Figure 3a shows a significant decrease of NO<sub>x</sub> emissions while speed increases between 0 and 70 km. Figure 3b demonstrates the significance of local meteorology on NO<sub>x</sub> emissions from a compact diesel sedan. Based on these NIER's CAPSS emission factors, the sensitivity to local ambient temperature is limited to NO<sub>x</sub> pollutant emissions from diesel vehicles.

Due to its high sensitivity to the vehicle operating speed, it is important for the CARS to simulate realistic speed patterns for accurate emissions estimates. When a single speed is assigned to compute hot exhaust emissions, it won't reflect the emissions under low-speed circumstances. To overcome this limitation, the CARS has adopted the 16 average speed bins concepts for a better representation of vehicle speed distribution that varies by road type (i.e., local, highway, expressway). We have implemented a feature for the CARS optionally to apply road-specific average speed distributions (ASD) ( $A_{bin,r}$ ), which represents the fractions of 16-speed bins (*bin*) (from 0 to 121 km h<sup>-1</sup> defined in Appendix E) for eight different road types (*r*) (No.101-108, shown in Appendix C) as classified by CAPSS (Fig. 4a). Although ASD patterns vary by region and time, current CARS model version does not support ASD application by region and time of day due to the lack of region and time dependent ASD availability in South Korea.

We first developed the ASD (Fig. 4a) for eight different road types (No. 101-108) in South Korea based on the latest road link-specific average speed and the length of link from the SK GIS road network shapefiles (NIER, 2018). Because the original link-level speed data is averaged, we used the link length as a weighting factor to show the variation of speed pattern for each link. However, the ASD based on the SK GIS road shapefiles wasn't able to capture the low-speed range (<16 km h<sup>-1</sup>) that occurs while it operates (Fig. 4a). It caused the significant underestimation of NO<sub>x</sub> and VOC emissions compared to the CAPSS (Appendix G).

To address this SK ASD issue, we incorporated the ASD (Figure 4b) from the state of Georgia developed by U.S. EPA to improve the representation of the low-speed ranges (speed bin #1 and #2 for road type 1 to 7). We increased the total fractions of low-speed bins (the 2:1 ratio of fractions of bin #1 and #2) by 2% for interstate expressways, 3% for urban expressways, 7% for all highways, and 15% for all local roads. The increases in low-speed bins lowered the distributions of other higher speed bins homogeneously due to the renormalization of fractions by road type. Figure 4c shows the renormalized hybrid-ASDs of all road types based on SK ASD and Georgia ASD. We understand, the hybrid-ASD approach is not ideal for SK onroad emission inventory development. However, it clearly demonstrates the CARS's capability and sensitivity to the vehicle speed representation and the impacts of ASD to the local onroad mobile inventories.

While 16-speed bins ASD application is critical to computing more realistic hot exhaust emissions, there should be some restrictions on certain road types. Users can adjust the restricted roads control table input file to limit the vehicle types that can only be operated on a particular road type. For example, motorcycles are limited to local roads (No. 104, 106, and 107), but not on expressways (No. 101, 102, 103, 105, and 108) due to its traffic regulation rules. Heavy trucks are



only allowed on the highway (No. 101, 102, 103, 105, and 108.) by law. The details of the road restriction control table format can be found on the CARS's user's guide from the CARS Github website ([https://github.com/bokhaeng/CARS/tree/master/docs/User\\_Manual](https://github.com/bokhaeng/CARS/tree/master/docs/User_Manual)).

The 16-speed bins averaged speed distribution calculated by road type ( $A_{bin,r}$ ) and road type weight factors ( $\omega_{r,d}$ ) in a district ( $d$ ) from Eq. (13) are added to the CARS hot exhaust emissions equation (Eq. 3). The hot exhaust emissions from individual vehicles ( $E_{hot;p,vin,myr}$ ) can be calculated by considering road-specific speed bins distribution (Eq. 5). Although the vehicles may be operated in different districts from their registered district, this is our best method to estimate the vehicle speed for hot exhaust emissions.

$$E_{hot;p,vin,myr} = DF_{p,v,myr} \times \sum_{bin} (VKT_{vin} \times EF_{hot;p,v,myr,s} \times A_{bin,r}) \quad (5)$$

## 2.2.2 Cold Start Emissions

The cold start emissions occur when a cold-engine vehicle is ignited. The lower temperature of the ICE is not an optimal condition for complete fuel combustion. This process lowers the combustion efficiency (CE) and increases the emissions of hydrocarbon and CO pollutants from the tailpipe exhaust (Jang et al., 2007). The CARS can estimate the cold start emissions for vehicles using gasoline, diesel, or liquefied petroleum gas (LPG) fuel. Besides the vehicle and engine type, road type also plays a critical role in the quantity of cold start emissions because it occurs mostly in parking lots and rarely on highways.

The cold start emission,  $E_{cold}$  (g d<sup>-1</sup>), is derived from the hot exhaust emissions, the ratio of hot to cold exhaust emissions ( $EF_{cold}/EF_{hot} - 1.0$ ), and the percentage of the traveled distance with a cold engine (Eq. 6).

$$E_{cold;p,v} = \beta_T \times E_{hot;p,v} \times \left( \frac{EF_{cold;p,v}}{EF_{hot;p,v}} - 1.0 \right) \quad (6)$$

The emission factor of cold start emissions ( $EF_{cold}$ ) is not directly calculated from measurement data like hot exhaust emissions ( $E_{hot;p,v}$ ), but measured under different ambient temperatures ( $T$ ). The CARS model applies linear regression models developed by CAPSS to estimate the increasing ratio of cold start to hot exhaust emissions ( $EF_{cold}/EF_{hot}$ ) under different temperatures ( $T$ ) (Eq. 7). In this equation,  $A$  and  $B$  are the empirical coefficients that vary by the pollutants ( $p$ ) and vehicle type ( $v$ ).

$$\left( \frac{EF_{cold;p,v}}{EF_{hot;p,v}} \right) = A_{p,v} + B_{p,v} \times T \quad (7)$$

$\beta$  is the percentage of the distance traveled under a cold engine. It also depends on the ambient temperature. Cold ambient temperatures cause a longer distance traveled under a cold

engine due to the slower heating time. According to the CAPSS database for Seoul city (Lee et al., 2011a), the empirical linear equation for  $\beta$  is shown in Eq. (8). This formula represents how ambient temperature affects  $\beta$ . For example, when the average temperature is -2°C,  $\beta$  is 34.8%. In summer, the monthly average temperature is 25.7°C, which causes  $\beta$  to drop to 21%.

$$\beta = 0.647 - 0.025 \times 12.35 - (0.00974 - 0.000385 \times 12.35) \times T \quad (8)$$

### 2.2.3 Evaporative VOC Emissions

Evaporative emissions are emissions from vehicle fuel that are evaporated into the atmosphere. This occurs in the fueling system inside the vehicle, such as fuel-tanks, injection systems, and fuel lines. Diesel vehicles, however, can be exempted due to diesel fuel's low vapor pressure. The primary sources of evaporative emissions are breathing losses through tank vents and fuel permeation/leakage. The CARS model adopted the EEA's emission inventory guidebook (EEA, 2019) to account for three mechanisms to estimate the evaporative VOC emissions ( $E_{vap}$ ): diurnal emissions from the tank ( $e_d$ ), hot and warm soak emissions by fuel injection type ( $S_{fi}$ ), and running loss emissions ( $R$ ) (Eq. 9). Unlike CAPSS, there is a conversion factor (0.075) applied to  $E_{vap}$  for motorcycles to prevent an over-estimation of VOC.

$$E_{vap;p,v} = (e_{d;p,v} + S_{fi;p,v} + R_{l;p,v}) \quad (9)$$

Diurnal emissions,  $e_d$  (g d<sup>-1</sup>), during the daytime are caused by the ambient temperature increase and the expansion of fuel vapors inside the fuel tank. Most of the current fuel tank systems have emission control systems to limit this kind of evaporative VOC emissions. The  $e_d$  can be calculated with the empirical Eq. (10), which was developed by CAPSS.  $T_l$  is the monthly average of the daily lowest temperatures and  $T_h$  is the monthly average of the daily highest temperatures. The empirical coefficient  $\alpha$  is 0.2, which represents how 80% of emissions are eliminated by the vehicle emission control system.

$$e_d = \alpha \times 9.1 \exp [0.3286 + 0.0574 \times (T_l) + 0.0614 \times (T_h - T_l - 11.7)] \quad (10)$$

Soak emissions ( $S_{fi}$ ) occur when a hot ICE is turned off; the remaining heat from the ICE can increase the fuel temperature in the system. The carburetor float bowls are the major source of the soak emissions. Newer vehicles with fuel injection and return-less fuel systems do not emit soak emissions. Because most of the current vehicles in South Korea have a new fuel system, soak emissions ( $S_{fi}$ ) in the CARS model are set to 0.

The running loss emissions ( $R_l$ ) are from vapors generated in the fuel tank when a vehicle is in operation (Eq. 11). In some older vehicles, the carburetor and engine operation can increase the temperature in the fuel tank and carburetor, which can cause a significant increase in evaporative VOC emissions. VOC emissions from running loss can be greatly increased during

warmer weather. However, newer vehicles with fuel injection and return-less fuel systems are not affected by the ambient temperature. Because most vehicles in South Korea do not use carburetor technology, we expect running loss emissions to have the least impact (Lee et al., 2011b).

$$R_l = \alpha \times L_{r,v} \times [(1 - \beta) \times R_h + \beta \times R_w] \quad (11)$$

The empirical coefficient  $\alpha$  is 0.1 here, which represents that 90% of the running loss is avoided by the newer fuel system.  $L$  is the distance traveled (km) by road and is the same one used in hot exhaust emission calculations.  $\beta$  is the same parameter from Eq. (8). The  $R_h$  and  $R_w$  are the average emission factors from running loss under hot and warm/cold conditions, respectively.

### 2.3 Road Link-Level Emissions Calculations

In general, district-level automobile emissions calculations are driven by district-level averaged vehicle activity and operating data, which do not reflect realistic spatial patterns of onroad automobile emissions. The CARS model introduces road link-specific traffic data by default to develop spatially enhanced road link-specific emissions that reflect more representative emissions by road link. This high-resolution traffic data is a GIS shapefile that is composed of many connected segments, which are called “road links.” All road links hold information such as start/end location coordinates, AADT, road link length, averaged vehicle speed, and road type (No. 101-108).

The CARS model applies link-level AADT ( $AADT_{d,r,l}$ ,  $d^{-1}$ ) and road length ( $L_{d,r,l}$ ) to compute the road link-specific VKT ( $VKT_{d,r,l}$ ,  $km\ d^{-1}$ ) in Eq. (12). The road links are identified by district ( $d$ ), road type ( $r$ ), and link ( $l$ ) labels. The road VKT is a parameter that reflects the traffic activity of each road link and it is different from individual daily vehicle activity data ( $VKT_{v,age}$ ) in Eq. (1).

$$VKT_{d,r,l} = AADT_{d,r,l} \times L_{d,r,l} \quad (12)$$

Road link-specific VKT ( $VKT_{d,r,l}$ ) is used to redistribute the district total emissions ( $E_{onroad}$ ) from Eq. 2 into road link-level emissions. The following three weight factors are computed: the district weight factors,  $\omega_d$  (Eq. 13), the road type weight factors,  $\omega_{d,r}$  (Eq. 14), and the road-link weight factors,  $\omega_{d,l}$  (Eq. 15). The weight district factors ( $\omega_d$ ) are the renormalization of each district's total VKT over state-level total VKT ( $N$  is the number of districts). The main reason we performed the renormalization over state-level total VKT is to reflect daily traffic patterns from multiple districts under the assumption that most vehicles travel within the same state. The road type weight factors by district ( $\omega_{r,d}$ ) are used to compute road-specific emissions, while road-specific averaged speed distributions (ASD;  $A_{s,r}$ ) from Eq. (5) are applied to capture vehicle

operating speeds by road type. The road link weight factors ( $\omega_{d,l}$ ) are then applied to redistribute the district emissions into road link-level emissions.

$$\omega_d = \frac{\sum_r \sum_l VKT_{d,r,l}}{\frac{1}{N} \sum_d \sum_r \sum_l VKT_{d,r,l}} \quad (13)$$

$$\omega_{d,r} = \frac{\sum_l VKT_{d,r,l}}{\sum_r \sum_l VKT_{d,r,l}} \quad (14)$$

$$\omega_{d,l} = \frac{VKT_{d,r,l}}{\sum_r \sum_l VKT_{d,r,l}} \quad (15)$$

### 3 CARS Configuration

The CARS model is an open-source program based on Python (Guido van Rossum, 2009) that allows the users to efficiently apply open-source modules to develop programs. Users can easily install Python development tools and load customized packages and modules to set up the CARS development environment. All CARS modules are developed using Python v3.6. Other than the GIS road shapefiles, all input files are based in the ASCII CSV format, which can be easily handled by both spreadsheet programs and programming languages, making it more accessible for users of all skillsets. The CARS can not only estimate district-level and spatially enhanced road link-level emissions, but can also generate hourly chemically speciated gridded emissions for CTMs. In addition, the CARS also generates various summary reports, graphics, and georeferenced plots for quality assurance.

The required Python modules for the CARS are: “*geopandas*,” “*shapely.geometry*,” and “*csv*” modules to read the shapefiles and table data files. The “*NumPy*” and “*pandas*” modules are used to operate the memory arrays and scientific calculations while the “*pyproj*” module deals with converting the projection coordinate systems. “*matplotlib*” is for generating any type of figures/plots. Furthermore, the CARS model can also read and write Climate and Forecast (CF)-compliant NetCDF-formatted files using “*NetCDF4*”.

The first process in the CARS is “*Loading\_function\_path*”; it allows users to define and check the input file paths. Once all input files are checked, there are six process modules in CARS to process inputs, compute emissions, and generate various output files, including QA reports. Figure 5 is the schematic of the CARS that consists of six process modules with various functions. The six process modules are (1) “**Process activity data**”, (2) “**Process emission factors**”, (3) “**Process shapefile**”, (4) “**Calculate district emissions**”, (5) “**Grid4AQM**”, and (6) “**Plot figures**”. The main purpose of modularizing the CARS is to meet the needs of various communities, such as policymakers, stakeholders, and air quality modelers. While modules (1) through (4) are required to develop the district-level and road link-level emissions inventories, module (5)

“Grid4AQM” is optional depending on if users want to develop chemically-speciated gridded hourly emissions for CTMs. Also, the modularity system in the CARS allows users to bypass certain modules if it has been previously processed without any changes. For example, if there is no change in traffic activity, emission factors table, or GIS shapefiles, users do not need to run these modules and can simply read the data frame outputs and then run “Grid4AQM” for the modeling dates and domain. The “Grid4AQM” module will not only improve the computational time for CTMs but also eliminate the need for a 3<sup>rd</sup> party emissions modeling system like SMOKE (Baek and Seppanen, 2021).

The rectangle boxes in Fig. 5 represent the data array and the boxes with rounded edges are the functions in the CARS. Details on the CARS code, input table format, and functions setup information can be found on the CARS GitHub website (Pedruzzi *et al.*, 2020).

The “Process activity data” module first reads the vehicle activity data, such as an individual vehicle's daily total VKT based on its registered district. The “Process emission factors” module reads and stores the emission factors table that holds all pollutant emission factors to estimate the emissions for all vehicles. Meteorology-sensitive emission factors are only limited to NO<sub>x</sub> pollutants. District boundary GIS shapefiles and road network shapefiles are processed through “Process shape file” to generate the VKT-based redistribution weighting factors from Eq. (13), (14) and (15) for the “Calculate district emissions” module to compute district-level and road link-level emission rates (metric tons per year, t yr<sup>-1</sup>).

The redistributed emission rates (t yr<sup>-1</sup>) from the “Calculate district emissions” module present annual total emission rates until district-level VKTs from the “Process activity data” module are added. Then, the “Grid4AQM” module can generate CTM-ready chemically speciated emissions. The “Read\_chemical” function from the “Grid4AQM” module is designed to process the chemical speciation profile that can convert the inventory pollutants such as CO, NO<sub>x</sub>, SO<sub>2</sub>, PM<sub>10</sub>, PM<sub>2.5</sub>, VOC, and NH<sub>3</sub>, into the chemically lumped model species that CTM requires for chemical mechanisms, such as SAPRC (L. and Heo, 2012) and Carbon Bond version 6 (CB6) (Yarwood and Jung, 2010). The “Read\_temporal” function processes the complete set of monthly, weekly, and hourly temporal allocation profiles that can convert annual total emissions to hourly emissions. “Read\_griddesc” defines the CTM-ready modeling domain and computes the gridding fractions for all road link-level emissions by overlaying the modeling domain over the GIS shapefiles. Once annual total emissions are chemically speciated, spatially gridded, and temporally allocated into hourly emissions, the “Gridded\_emis” function will combine emission source-level conversion fractions from each function (*Read\_chemical*, *Read\_temporal*, and *Read\_griddesc*) to generate the CTM-ready chemically speciated, gridded hourly emissions in the NetCDF binary format. The “Plot Figures” module is designed for generating various summary reports and graphics to assist users in understanding the estimated automobile emissions inventory computed by the CARS. The following section will describe the detailed processes of the “Grid4AQM” module, which includes chemical, spatial, and temporal allocations.

The influence of temperature on emission processes are considered in the CARS model. There are three temperature parameters in current CARS model such as “temp\_max” for maximum temperature, “temp\_mean” for mean temperature, and “temp\_min” for minimum temperature. These temperature parameters will be applied to over the entire modeling domain during the simulation period. Current CARS model version does not support to process gridded meteorology data from the 3<sup>rd</sup> party meteorology models like Meteorology-Chemistry Interface Processor (MCIP) from U.S. EPA., and Weather Research Forecasting (WRF) model from National Center for Atmospheric Research (NCAR) yet. However, CARS can easily adopt various temporally resolved temperature values by adjusting the CARS simulation period (i.e., day, week, month, season, or annual).

### 3.1 Chemical Speciation

To support CTMs applications, the CARS needs to be able to convert inventory pollutants into chemical lumped model species based on the choice of CTM chemical mechanisms. NO<sub>x</sub> includes nitric oxide (NO), nitrogen dioxide (NO<sub>2</sub>), and nitrous acid (HONO). VOCs can represent hundreds of different organic carbon species, such as benzene, acetaldehyde, and formaldehyde. These grouped inventory pollutants cannot be directly imported into the chemical mechanism modules in the CTM system and require chemical speciation allocation for CTMs to process them during their chemical reactions. Therefore, the “**Grid4AQM**” module performs the chemical species allocation step prior to the temporal and spatial allocations to generate the gridded hourly emissions. The “**Read\_chemical**” function in “**Grid4AQM**” module allows users to assign these emission inventory pollutants to CTM-ready surrogate chemical species (a.k.a lumped chemical species) by vehicle, engine, and fuel type. For example, VOC emissions from diesel busses can be converted into the following composition based on its chemical allocation profile: alkanes (68%), toluene (9%), xylenes (8%), alkenes (4%), ethylene (2%), benzene (1.3%), and unreactive compounds (7%) when CB6 chemical mechanism is selected. Further details on the chemical speciation profile input formats are available in the CARS user’s guide.

### 3.2 Spatial Allocation

The “**Calculate district emissions**” module calculates not only the total district emissions but also road link-specific emissions based on road link-specific AADT data from road network GIS shapefiles. The “**Calculate district emissions**” module first gets the district total vehicle emissions (Eq. 2) based on the district-level VKTs, and then the normalized district total emissions by district weight factor,  $\omega_d$  (Eq. 13). Afterwards, the normalized district total emissions are redistributed into every road link using road link-level weight factors ( $\omega_{d,l}$ ) (Eq. 15). The district total emissions from Eq. (2) and from Eq. (15) remain the same. Then the computed road link-



level emissions then will be converted into grid cell emissions using the modeling domain grid cell fractions computed in the “*Read\_griddesc*” function in the “**Grid4AQM**” module.

### 3.3 Temporal Allocation

Once chemical and spatial allocations are completed, the final step to support CTM application is a temporal allocation that converts the annual total emissions from the “**Calculate district emissions**” module into hourly emissions. The “*Read\_temporal*” temporal allocation function in the “**Grid4AQM**” module converts the annual emission rate ( $\text{t yr}^{-1}$ ) to the hourly emission rate ( $\text{mol hr}^{-1}$ ) using monthly, weekly, and weekday/weekend diurnal temporal profiles. This module processes these temporal profile inputs, which are the monthly (January - December), weekly (Monday - Sunday), and weekday/weekend 24 hour profile tables (0:00-23:00 LST). The users can assign these temporal profiles with a combination of vehicle, engine, fuel, and road types to enhance their temporal representations in detail.

### 3.4 Chemical Transport Model Emissions

The main goal of the “**Grid4AQM**” module is to generate temporally, chemically, and spatially enhanced CTM-ready gridded hourly emissions. First, it reads the CTM modeling domain configuration and then overlays it over the road network GIS shapefile and district-boundary shapefile to define the modeling domain. This overlaying process between the road network, district boundary GIS shapefiles, and modeling domain allows the “**Grid4AQM**” module to compute the fraction of road links that intersects with each grid cell. Figure 6 demonstrates how the district boundary and road network GIS shapefiles are used to perform the spatial allocation processes in CARS. Figure 6a is a native road link shapefile of Seoul with AADT, VKT, district ID, and road type. Figure 6b presents an overlay of two districts’s road links (purple and blue) over the selected region. State total emissions will be renormalized into weighed district total emission data and then redistributed into the road link. Figure 6c illustrates how the weighted road link-level emissions get allocated into modeling grid cells for CTMs. The link-level VKT ( $VKT_{d,r,l}$ ) from Eq. (12) will be used to compute a total of traffic activity fractions by grid cell and then use that to assign the link-level emissions from Eq. (2) into each grid cell. When a road link intersects with multiple grid cells, the “**Grid4AQM**” module will weigh the emissions by the length of the link that intersects with each grid cell. It should be noted that current CARS model can only generate the Community Multiscale Air Quality (CAMQ)-ready gridded hourly emissions in format of IOAPI (Input/Output Applications Programming Interface) based on NetCDF format.

Through the overlay process, the CARS model can generate various types of output data, such as total district emissions, link-level emissions, and CTM-ready gridded emissions. For example, the CO vehicle emissions from the Seoul metropolitan in South Korea are presented in three different output formats in Fig. 7. Figure 7a shows the annual mobile  $\text{PM}_{2.5}$  emissions by

district. The road link level annual emissions are presented in Fig. 7b. Furthermore, the CARS applies the link-level emissions from Fig. 7b to generate the hourly grid cell emission data with a 1 km × 1 km resolution for the CTM in Fig. 7c.

### 3.5 National Control Strategy Application

One of the unique features in the CARS compared to other mobile emissions models is that it can promptly develop controlled mobile emissions responding to the national emergency high PM<sub>2.5</sub> episodes. It is very common to experience high PM<sub>2.5</sub> episodes, especially during the wintertime in South Korea due to domestic and international primary and secondary air pollutants emissions. When the 72 hour forecasted PM<sub>2.5</sub> concentration exceeds the average 50 µg/m<sup>3</sup> (0:00-16:00 LST), the national PM<sub>2.5</sub> emergency control strategy is activated for ten days. It applies a nationwide vehicle restriction policy within 24 hours. It enforces a limit on what kind of vehicles can be operated on a certain date. The restrictions can be applied in the following ways: the closures of public parks and government facilities, and restrictions of certain vehicles based on their fuel type and age, which is a major factor of engine deterioration. This policy will limit the number of vehicles on the network roads significantly, which could reduce primary PM<sub>2.5</sub> and precursor pollutant (NO<sub>x</sub>, NH<sub>3</sub>, and VOC) emissions, especially from heavily populated metropolitan regions (Choi et al., 2014; Kim et al., 2017a; Kim et al., 2017b; Kim et al., 2017c).

To understand the impacts of an even/odd vehicle restriction policy in real-time, we need to quickly develop a rapid control response emissions for the air quality forecast modeling system. The process of generating the controlled mobile emissions can take a long time if we start fresh. Thus, we have implemented this control strategy as an optional “**Control Factors**” function in the “**Calculate district emissions**” in the module for users to quickly and easily generate the controlled mobile emissions with consideration of the limited number of vehicles based on the vehicle, engine, fuel, and vehicle manufactured year. A one hundred percent (100%) control factor means that there are no emissions from those selected vehicles.

Because of the modularization system in the CARS, we can bypass some computationally expensive data processing modules (i.e., “**Process activity data**”, “**Process emission factors**”, and “**Process shape file**”) and let the “**Calculate district emissions**” module quickly apply control factors while it computes the district-level mobile emission inventory from Eq. (2). This will allow users to reduce the computational time to generate the controlled mobile emissions under a specific control scenario and develop the controlled CTM-ready gridded hourly emissions using the “**Grid4AQM**” module.

### 3.6 Computational Time

While the CARS can generate a high-quality spatiotemporal emission inventory for policymakers, stakeholders, and air quality modelers, it is quite critical for the CARS to generate

these complex mobile emissions effectively and accurately without being at the expense of computational time. This is especially important to meet the needs for an air quality forecast modeling system responding to a national emergency control strategy implementation.

In this section, we will discuss the details of the CARS computational modeling performance. While the CARS model has been highly optimized, the modularization of CARS has also improved its modeling performance with optional module runs. The breakdown of module-specific computational time estimates based on the benchmark CARS runs are listed in Table 1. The benchmark CARS case includes a total of 24,383,578 daily VKT datasets from KSTA over two different years, 84,608 emission factors for all pollutants across a combination of vehicle-age-engine-fuel types, 385,795 road links from the GIS road network shapefiles, 5,150 districts/16-states boundary GIS shapefile, and 5,494 grid cells (=82 rows and 67 columns) for CTMs. Without any computational parallelization, the total processing time of all six modules usually takes around a half hour to generate a single day CTM-ready gridded hourly emission file. However, it can be further shortened to 25-30 minutes on a higher performance computer. Because of the modular system implemented in the CARS, generating one month (31 days) long gridded hourly emissions from CTMs do not require over 15 computational hours, but only around 100 minutes on high-performance computers. The maximum usage of RAM can reach up to 11 GB. Table 1 shows the breakdown of computational time by each module from two different hardwares (desktop and laptop computers). The numbers in parentheses beside the “Grid4AQM” module is the computational time for a single day versus 31 days. While the “Grid4AQM” module takes an average of 4.9 minutes for a single day emissions generation, processing a consecutive 31 days saves 46% more time, decreasing from 151.9 minutes (=4.9 minutes \* 31 days) to 81.6 minutes.

## 4 Results

### CARS and CAPSS Comparison

The CARS model calculates the 2015 onroad automobile emissions based on the latest 2015 emission factors and the 2015-2017 vehicle activity database in South Korea. The annual total emissions from CARS are compared against the ones from NIER CAPSS in Table 2. The CARS model estimated the following annual total emissions in units of metric tons per year (t yr<sup>-1</sup>): NO<sub>x</sub> (301,794); VOC (61,186); CO (373,864), NH<sub>3</sub> (12,453); PM<sub>2.5</sub> (10,108), and SO<sub>x</sub> (172.0). Compared to NIER CAPSS, the CARS overestimated all pollutants except for NO<sub>x</sub> (-18% decrease) and SO<sub>x</sub> (-17% decrease). It overestimated the emissions of VOC by 33%, PM<sub>2.5</sub> by 15%, CO by 52%, and NH<sub>3</sub> by 24%. Both NIER CAPSS and CARS shared the same emission factor tables, which hold over 84,608 emission factors for all pollutants across a combination of vehicle, age, engine, and fuel types.

The difference between CAPSS and CARS approaches are caused by three reasons: First, the number of vehicles used in CARS is slightly higher (6%) than CAPSS data (1.3 out of 23

million), as well as other key traffic-related activity inputs (i.e., vehicle age distribution, averaged speed distribution, etc). Secondly, the vehicle speed information assigned by vehicle and road type play a critical role in the differences between CAPSS and CARS. The CAPSS calculation was based on the road-specific mean speed value or 80% of the speed limit as an input of vehicle operating speed by three road types (rural, urban, and expressway). In other words, CAPSS only assigns a “single-speed value” for each road type, and does not encounter the variation of vehicle speed during its operation on roads into the emissions calculation. Most running exhaust emissions occur during a vehicle’s low-speed operation due to its incomplete combustion of fuel, and it is critical to accurately represent the emissions across various speed bins in order to compute the correct emissions. The CARS model has an option to apply the average speed distribution (ASD) over 16 speed bins for eight road types (Fig. 4). The CARS speed distribution process can better represent the speed variations of vehicle speeds for each road type. A detailed analysis of the impact of vehicle speed will be discussed later in this chapter. Lastly, other advanced processes in the CARS, such as link-level AADT and district-level vehicle data (5,150 districts in South Korea), can reflect more spatial detail and variation than the CAPSS. The CAPSS only considers state-level data (17 states in South Korea) and five road types (interstate expressway, urban highway, rural highway, urban local, and rural local).

Figure 8 illustrates more details about the difference between the annual emissions from CARS to the CAPSS by pollutants and vehicle types. Sedan vehicles show the largest increase of VOC (33%), CO (41%), and NH<sub>3</sub> (23%) in the CARS relative to CAPSS because almost 56% of total vehicle count (13.5 million) is composed of sedan vehicles. Also, sedan vehicles contribute 51% of total VOC and 61% of total CO annual emissions. The VOC and CO emissions from sedans are largely affected by the average speed distribution process when compared to other vehicle types. Similarly, the largest decreases of NO<sub>x</sub> (-16%) and SO<sub>x</sub> (-18%) are from trucks because they are significant NO<sub>x</sub> (~50%) and SO<sub>x</sub> contributors (~27%) and their emission factors are sensitive to vehicle speed.

## **Onroad Emissions Analysis**

The CARS is a bottom-up emissions model, which utilizes local individual vehicle activity data, detailed local emission factors for every vehicle and fuel type, and localized inputs such as average speed distribution by road type and deterioration factor. It allows users to assess the detailed breakdown of localized emission contributions. Table 3 represents the individual air pollutants (NO<sub>x</sub>, VOC, PM<sub>2.5</sub>, CO, NH<sub>3</sub>, and SO<sub>x</sub>) emission contributions (t yr<sup>-1</sup>), fractions (%), and impact factors (IF) by the vehicle type and fuel system. The IF is defined by the normalized annual emissions with vehicle counts of each category (kg yr<sup>-1</sup> per vehicle). The CARS also can provide the average daily VKT per vehicle, which is the total daily VKT divided by vehicle numbers, to explain the emission contributions in Appendix D.

Diesel-fueled vehicles contribute the most of  $\text{NO}_x$  emissions, which is over 85.3% (257,305 t  $\text{yr}^{-1}$ ), although the number of diesel vehicles only amounts to approximately 35% of the total vehicles (Table 3a). While the diesel trucks emitted 49.1% (148,246 t  $\text{yr}^{-1}$ ) of total  $\text{NO}_x$  with an IF value of 47.9 (kg  $\text{yr}^{-1}$ ), the highest impact (IF = 340 kg  $\text{yr}^{-1}$ ) occurred from diesel buses with only a 8.51% contribution to the total  $\text{NO}_x$  emissions. This is caused by the highest average daily VKT from diesel buses compared to other vehicles, which is expected in a highly populated metropolitan area like Seoul, South Korea. A diesel bus generally has a 3-5 times higher daily VKT (180 km  $\text{d}^{-1}$ ) than other common vehicles (gasoline sedan: 34 km  $\text{d}^{-1}$ , diesel truck: 57 km  $\text{d}^{-1}$ ). The second-largest vehicle type is the CNG (compressed natural gas) bus (248 kg  $\text{yr}^{-1}$ ), which also has a higher VKT. Their average daily VKT is 212 km  $\text{d}^{-1}$ , with only a 3.1%  $\text{NO}_x$  contribution.

For VOC emissions, over 12 million gasoline vehicles cause 52.1% (31,885 t  $\text{yr}^{-1}$ ) of the total VOC emissions, and the gasoline sedan is the highest contributor across all vehicle types, which is over 28,434 t  $\text{yr}^{-1}$  (46.5%) (Table 3b). Unlike  $\text{NO}_x$  emissions, diesel vehicles only contribute 23.0% (14,070 t  $\text{yr}^{-1}$ ) of the total VOC emissions. Across the vehicle fuel types, the IF outcome indicates that CNG vehicles have the highest IF values for VOC, which is 247 kg  $\text{yr}^{-1}$  due to the relatively high VOC contribution (19% over total VOC) and a low number of heavy CNG vehicles. The IF of CNG trucks are 77.2 kg  $\text{yr}^{-1}$ , but only contribute 0.2% to total VOC emissions. The IF of the CNG bus is 320 kg  $\text{yr}^{-1}$  and emits 19.5% of the total VOC. Comparing the IFs of buses across fuel types, the CNG bus emits less  $\text{NO}_x$  but higher VOC than a diesel vehicle. Each CNG bus has about 33 times higher IF of VOC (320 kg  $\text{yr}^{-1}$ ) than a diesel bus (9.51 kg  $\text{yr}^{-1}$ ), and CNG buses released slightly lower  $\text{NO}_x$  (248 kg  $\text{yr}^{-1}$ ) than diesel buses (340 kg  $\text{yr}^{-1}$ ) (Table 3a and 3b). It indicates that a CNG bus is better for rural areas and a diesel bus is better for urban areas to control ozone, because the rural area is usually  $\text{NO}_x$  limited for ozone formation and urban areas are VOC limited.

The current South Korea NIER currently does not have the PM emission factors from tire and brake wear, which are the highest contributors of  $\text{PM}_{2.5}$  emissions from onroad vehicles (Hugo A.C. et al., 2013; Fulvio Amato et al., 2014). Once the emission factors of tire and brake wear are prepared, those emissions can be computed by CARS. For that reason, diesel vehicles become the major source of  $\text{PM}_{2.5}$  emissions, which contributes over 98.5% (9,959 t  $\text{yr}^{-1}$ ) of the  $\text{PM}_{2.5}$  emissions based on the CARS 2015 emissions (Table 3c). The diesel truck, SUV, and van are the three major sources, and their contributions of total  $\text{PM}_{2.5}$  are 53.6%, 21.4%, and 11.2%, respectively. Although over 52% of the vehicles are gasoline vehicles, their primary  $\text{PM}_{2.5}$  contribution is limited to 1.44%. The diesel bus has the highest IF (2.83 kg  $\text{yr}^{-1}$ ), which is caused by the largest average daily VKTs.

Similar to VOC emissions, CO is mostly emitted through the tailpipe due to incomplete internal combustion of fuel and share similar emissions distributions across vehicle and fuel types (Table 3d). Gasoline vehicles contribute most of the CO (220,390 t  $\text{yr}^{-1}$ , 59.0%), and sedan vehicles are the primary source (178,121 t  $\text{yr}^{-1}$ , 47.6%) of this out of all gasoline vehicles. Across vehicle

types, bus shows the highest IF of CO (81.2 kg yr<sup>-1</sup>) due to its largest daily VKT. CO is the most abundant pollutant released from vehicles (373,864 t yr<sup>-1</sup>) across all pollutants from onroad automobile sources. Although CO is much less reactive than other vehicle VOCs (Rinke and Zetzsch, 1984; Liu and Sander, 2015), the majority of CO emissions from onroad automobile sources plays a critical role in generating 30% of hydroperoxyl radicals (HO<sub>2</sub>) and causing ozone formation in urban areas (Pfister et al., 2019). Thus, CO is also another crucial precursor to ozone formation in urban areas.

SO<sub>x</sub> emissions are related to the sulfur content within the fuel component; diesel has a higher sulfur content than any other fuels. Most SO<sub>x</sub> is contributed by diesel vehicles (93.8 t yr<sup>-1</sup>, 54.5%) (Table 3e). Within diesel vehicles, trucks provide 26.5% of SO<sub>x</sub> (45. t yr<sup>-1</sup>). Although the SO<sub>x</sub> from sedan vehicles are slightly higher (~3.3%) than diesel trucks, the number of diesel trucks is only 29.6% of the number of gasoline sedans. Thus, diesel trucks have a higher IF than gasoline sedans. Across vehicle types, buses have the highest IF (0.095 kg yr<sup>-1</sup>) of SO<sub>x</sub>, and diesel buses in particular have the largest IF at 0.143 kg yr<sup>-1</sup>.

The NH<sub>3</sub> emissions table (table 3f) indicates that 98.7% of NH<sub>3</sub> is from gasoline vehicles while diesel trucks only contribute 1.13%. The IF result also shows that the gasoline sedan has the most significant impact per vehicle (1.17 kg yr<sup>-1</sup>).

According to the vehicle activity and the CARS model results, nearly half of the total vehicles (24.3 million) are gasoline sedans (10.4 million, 42.8%), and gasoline sedan vehicles contributed most of the VOC and CO emissions (46.5% and 47.6%), but only 7.7% of the total NO<sub>x</sub> emissions. The number of diesel vehicles is 8.6 million (35.4%); however, they emitted about 85.3% of the total NO<sub>x</sub> and 98.5% of the primary PM<sub>2.5</sub>. These results indicated that the annual traffic-related mobile emissions are not only affected by the number of vehicles, but also by different vehicle and fuel types. Therefore, this study normalized the annual emissions by the number of vehicles to confirm the emission composition by individual vehicle types.

### **Average Speed Impact Study**

The CARS can also optionally apply the average speed distribution (ASD) by road type to compute more realistic mobile emissions on the road network when compared to using a current single average speed value for each road type (Appendix E). Applying the ASD will generate a much better representation of actual traffic patterns from each road type. To understand the impacts of ASD application, we performed sensitivity runs between using a single-speed to the ASD application (Appendix F). The ASD data was described in Fig. 4, and the road-specific average single-speed values were developed based on the weighted average method using the same ASD data. Appendix E and S6 describes the details of ASD as well as road-specific speed values.

Figure 9a shows the differences in total emissions between two scenarios and is organized by pollutant. The single-speed scenario largely underestimates the emissions across all pollutants compared to the ones from the ASD scenario. NO<sub>x</sub> (16%), VOC (40%), and CO (30%) were



especially underestimated. The difference is caused by the lack of low-speed bins ( $<16 \text{ km h}^{-1}$ ) representation when a single average speed approach was used. Higher emissions are emitted while vehicles are operated with low-speed bins, which decreases the combustion efficiency of ICE and releases more pollutants.

Figure 9b shows the road-specific breakdown between the ASD and single speed scenarios to understand the impacts of vehicle operating speeds on onroad automobile emissions. In this figure, each color indicates the emissions percentage differences by road types. Other than  $\text{NH}_3$ , significant discrepancies happened between local urban roads (5.8%), highways (3.9%), and urban highways (3.0%). Other pollutants, VOC,  $\text{PM}_{2.5}$ , CO, and  $\text{SO}_x$ , have similar fractions of road types. This phenomenon is caused by low-speed conditions ( $<16 \text{ km h}^{-1}$ ) and the fractions of road VKT contributions (Appendix C). The lower speeds cause the incomplete combustion of ICE and increase the emission rate. Also, local urban roads, highways, and urban highways have higher road VKT contributions at 17%, 18%, and 12%, respectively (Appendix C) than rural roads. Higher emissions from low speed conditions from these high contribution roads (urban local, urban highway, and highway) caused these significant differences between the ASD and single-speed approaches. Although the interstate expressway has the largest VKT contribution (41%), it also has the lowest fraction of low-speed bins (2%). That is why the difference between the ASD and single speed scenarios on interstate expressways is less than 1%. In general,  $\text{NH}_3$  emission factors do not change by vehicle operating speed, so the ASD impact is quite minimal.

## 5 Conclusions

The CARS is a bottom-up automobile emissions model that utilizes the localized traffic-related activity and emission factors input datasets to generate high quality localized bottom-up emissions inventories for policymakers, stakeholders, and research community as well as temporally and spatially enhanced hourly gridded emissions for CTMs. First, the CARS model employs the daily VKTs for all registered vehicles and the emission factors function to compute district-level total daily emissions for each vehicle. To reflect realistic traffic patterns, the CARS model computes and utilizes link-level VKTs ( $=\text{link-length} \times \text{AADT}$ ) from the road network GIS shapefiles to redistribute the original district-level total emissions into spatially enhanced road link-level emissions. It can also optionally implement a control strategy as well as road restriction rules to improve the quality of local emission inventories and meet the needs of users.

The CARS model is a fully modularized and computationally optimized python-based bottom-up mobile emissions model that can effectively process a huge dataset to calculate high quality spatiotemporal county-level, road link-level and grid cell-level mobile emissions. We believe that the implementation of the ASD into the CARS improves the representation of onroad automobile emissions from the road network when compared to a single-speed for each road type approach. It allows the CARS to have a better representation of low speed ( $<16 \text{ km h}^{-1}$ ) vehicle

emissions. We believe that CARS model's versatile spatiotemporal bottom-up automobile emissions and the in-depth analysis feature can assist government policymakers and stakeholders to develop the rapid responsive emission abatement strategies as a response to the South Korea's national PM<sub>2.5</sub> emergency control strategy that enforces the nationwide vehicle restriction policy within 24 hours.

### **Code Availability:**

The source code of the CARS model public release version 1.0 can be downloaded from the Github release website:

<https://github.com/bokhaeng/CARS/releases/tag/CARSv1.0>

### **Digital Object Identifier (DOI) for the CARS version 1.0:**

<https://zenodo.org/record/5033314#.YNzDrC1h001>

### **Installation Package for CARS version 1.0:**

The CARS version 1.0 installation package comes with the complete inputs and outputs datasets for users to confirm their proper installation on their computers and can be downloaded from the Github release website:

[https://github.com/bokhaeng/CARS/releases/download/CARSv1.0/CARS\\_v1.0\\_public\\_release\\_package\\_25June2021.zip](https://github.com/bokhaeng/CARS/releases/download/CARSv1.0/CARS_v1.0_public_release_package_25June2021.zip)

### **User's Guide Documentation:**

The CARS version user's guide documentation can be accessed through the Github repository:

[https://github.com/bokhaeng/CARS/tree/master/docs/User\\_Manual](https://github.com/bokhaeng/CARS/tree/master/docs/User_Manual)

### **Data availability:**

All the datasets, excel and python scripts used in this manuscript for the data analysis are uploaded through GMD website along with a supplemental appendix document.

## **Author contribution**

Dr. B.H. Baek and Dr. Jung-Hun Woo are lead researchers in this study. Dr. Rizzieri Pedruzzi develop the source code of CARS model, Dr. Minwoo Park tested the model and provided the model input data. Dr. Chi-Tsan Wang analyzed the model result and prepared the manuscript. Younha Kim, Chul-Han Song, analyzed the model result and provided comments.

## **Competing interests**

The Authors declare that they have no conflict of interest.

## **Acknowledgments**

This research was funded by the National Strategic Project-Fine Particle of the National Research Foundation (NRF) of Korea funded by the Ministry of Science and ICT (MSIT), the Ministry of Environment (ME), the Ministry of Health and Welfare (MOHW) (NRF-2017M3D8A1092022), and by the Korea Environmental Industry & Technology Institute (KEITI) through the Public Technology Program based on Environmental Policy Program, funded by Korea Ministry of Environment (MOE) (2019000160007).

## References

Safety flare for burning combustible gas - has tangential inlet for non-flammable gas between housing and stack, in, Shell Oil Co (Shel-C).

Anaconda, Anaconda python: <https://www.anaconda.com/products/individual>, last access: May, 1st, 2020.

Appel, W., Chemel, C., Roselle, S., Francis, X., Hu, R.-M., Sokhi, R., Rao, S. T., and Galmarini, S.: Examination of the Community Multiscale Air Quality (CMAQ) model performance over the North American and European domains, *Atmospheric Environment*, 53, 142–155, 10.1016/j.atmosenv.2011.11.016, 2013.

Baek, B. H., and Seppanen, C., SMOKE v4.8.1 Public Release (January 29, 2021) (Version SMOKEv481\_Jan2021): <http://doi.org/10.5281/zenodo.4480334> last 2021.

Burnett, R., Chen, H., Szyszkowicz, M., Fann, N., Hubbell, B., Pope, C. A., Apte, J. S., Brauer, M., Cohen, A., Weichenthal, S., Coggins, J., Di, Q., Brunekreef, B., Frostad, J., Lim, S. S., Kan, H., Walker, K. D., Thurston, G. D., Hayes, R. B., Lim, C. C., Turner, M. C., Jerrett, M., Krewski, D., Gapstur, S. M., Diver, W. R., Ostro, B., Goldberg, D., Crouse, D. L., Martin, R. V., Peters, P., Pinault, L., Tjepkema, M., van Donkelaar, A., Villeneuve, P. J., Miller, A. B., Yin, P., Zhou, M., Wang, L., Janssen, N. A. H., Marra, M., Atkinson, R. W., Tsang, H., Quoc Thach, T., Cannon, J. B., Allen, R. T., Hart, J. E., Laden, F., Cesaroni, G., Forastiere, F., Weinmayr, G., Jaensch, A., Nagel, G., Concin, H., and Spadaro, J. V.: Global estimates of mortality associated with long-term exposure to outdoor fine particulate matter, *Proceedings of the National Academy of Sciences*, 115, 9592, 10.1073/pnas.1803222115, 2018.

Choi, D., Beardsley, M., Brzezinski, D., Koupal, J., and Warila, J.: MOVES Sensitivity Analysis: The Impacts of Temperature and Humidity on Emissions, available at: <https://www3.epa.gov/ttn/chief/conference/ei19/session6/choi.pdf> 2017.

Choi, K.-C., Lee, J.-J., Bae, C. H., Kim, C.-H., Kim, S., Chang, L.-S., Ban, S.-J., Lee, S.-J., Kim, J., and Woo, J.-H.: Assessment of transboundary ozone contribution toward South Korea using multiple source–receptor modeling techniques, *Atmospheric Environment*, 92, 118–129, <https://doi.org/10.1016/j.atmosenv.2014.03.055>, 2014.

Cohen, A. J., Brauer, M., Burnett, R., Anderson, H. R., Frostad, J., Estep, K., Balakrishnan, K., Brunekreef, B., Dandona, L., Dandona, R., Feigin, V., Freedman, G., Hubbell, B., Jobling, A.,

- 814 Kan, H., Knibbs, L., Liu, Y., Martin, R., Morawska, L., Pope, C. A., III, Shin, H., Straif, K.,  
815 Shaddick, G., Thomas, M., van Dingenen, R., van Donkelaar, A., Vos, T., Murray, C. J. L., and  
816 Forouzanfar, M. H.: Estimates and 25-year trends of the global burden of disease attributable to  
817 ambient air pollution: an analysis of data from the Global Burden of Diseases Study 2015, *The*  
818 *Lancet*, 389, 1907-1918, 10.1016/S0140-6736(17)30505-6, 2017.
- 819
- 820 Dennis, R., Fox, T., Fuentes, M., Gilliland, A., Hanna, S., Hogrefe, C., Irwin, J., Rao, S. T.,  
821 Scheffe, R., Schere, K., Steyn, D., and Venkatram, A.: A FRAMEWORK FOR EVALUATING  
822 REGIONAL-SCALE NUMERICAL PHOTOCHEMICAL MODELING SYSTEMS, *Environ*  
823 *Fluid Mech (Dordr)*, 10, 471-489, 10.1007/s10652-009-9163-2, 2010.
- 824 EEA: EMEP/EEO air pollutant emission inventory guidebook 2016, 2019.
- 825 Enthought, Enthought Canapy Python: <https://assets.enthought.com/downloads/edm/>, last  
826 access: May, 1st, 2020.
- 827 Fallahshorshani, M., André, M., Bonhomme, C., and Seigneur, C.: Coupling Traffic, Pollutant  
828 Emission, Air and Water Quality Models: Technical Review and Perspectives, *Procedia - Social*  
829 *and Behavioral Sciences*, 48, 1794-1804, <https://doi.org/10.1016/j.sbspro.2012.06.1154>, 2012.
- 830 Fulvio Amato, Flemming R. Cassee, Hugo A.C. Denier van der Gon, Robert Gehrig, Mats  
831 Gustafsson, Wolfgang Hafner, Roy M. Harrison, Magdalena Jozwicka, Frank J. Kelly,  
832 TeresaMoreno, Andre S.H. Prevot, Martijn Schaap, Jordi Sunyer, Xavier Querol, Urban air  
833 quality: The challenge of traffic non-exhaust emissions, *Journal of Hazardous Materials*, 275, 31-  
834 36, <https://doi.org/10.1016/j.jhazmat.2014.04.053>, 2014.
- 835
- 836 Guevara, M., Tena, C., Porquet, M., Jorba, O., and Pérez García-Pando, C.: HERMESv3, a  
837 stand-alone multi-scale atmospheric emission modelling framework – Part 1: global and regional  
838 module, *Geosci. Model Dev.*, 12, 1885-1907, 10.5194/gmd-12-1885-2019, 2019.
- 839 Hogrefe, C., Rao, S. T., Kasibhatla, P., Hao, W., Sistla, G., Mathur, R., and McHenry, J.:  
840 Evaluating the performance of regional-scale photochemical modeling systems: Part II—ozone  
841 predictions, *Atmospheric Environment*, 35, 4175-4188, [https://doi.org/10.1016/S1352-](https://doi.org/10.1016/S1352-2310(01)00183-2)  
842 [2310\(01\)00183-2](https://doi.org/10.1016/S1352-2310(01)00183-2), 2001a.
- 843 Hogrefe, C., Rao, S. T., Kasibhatla, P., Kallos, G., Tremback, C. J., Hao, W., Olerud, D., Xiu,  
844 A., McHenry, J., and Alapaty, K.: Evaluating the performance of regional-scale photochemical

845 modeling systems: Part I—meteorological predictions, *Atmospheric Environment*, 35, 4159-  
846 4174, [https://doi.org/10.1016/S1352-2310\(01\)00182-0](https://doi.org/10.1016/S1352-2310(01)00182-0), 2001b.

847 Hugo A.C. Denier van der Gon, Miriam E. Gerlofs-Nijland, Robert Gehrig, Mats Gustafsson,  
848 Nicole Janssen, Roy M. Harrison, Jan Hulskotte, Christer Johansson, Magdalena Jozwicka,  
849 Menno Keuken, Klaas Krijgheld, Leonidas Ntziachristos, Michael Riediker & Flemming R.  
850 Cassee: The Policy Relevance of Wear Emissions from Road Transport, Now and in the  
851 Future—An International Workshop Report and Consensus Statement, *Journal of the Air &*  
852 *Waste Management Association*, 63:2, 136-149, DOI: 10.1080/10962247.2012.741055, 2013  
853

854 Ibarra-Espinosa, S., Ynoue, R., amp, apos, Sullivan, S., Pebesma, E., Andrade, M. d. F., and  
855 Osses, M.: VEIN v0.2.2: an R package for bottom-up vehicular emissions inventories, *Geosci.*  
856 *Model Dev.*, 11, 2209-2229, 10.5194/gmd-11-2209-2018, 2018a.

857 Ibarra-Espinosa, S., Ynoue, R., O'Sullivan, S., Pebesma, E., Andrade, M. D. F., and Osses, M.:  
858 VEIN v0.2.2: an R package for bottom-up vehicular emissions inventories, *Geosci. Model Dev.*,  
859 11, 2209-2229, 10.5194/gmd-11-2209-2018, 2018b.

860 IEMA, Inventário de Emissões Atmosféricas do Transporte Rodoviário de Passageiros no  
861 Município de São Paulo.: <http://emissoes.energiaeambiente.org.br>, last access: May,1st, 2017.

862 Jang, Y. K., Cho, K. L., Kim, K., Kim, H. J., and Kim, J.: Development of methodology for  
863 estimation of air pollutants emissions and future emissions from on-road mobile sources.,  
864 National Institute of Environmental Research, Incheon, Korea., available at: 2007.

865 Kaewunruen, S., Sussman, J. M., and Matsumoto, A.: Grand Challenges in Transportation and  
866 Transit Systems, *Frontiers in Built Environment*, 2, 10.3389/fbuil.2016.00004, 2016.

867 Kim, B.-U., Bae, C., Kim, H. C., Kim, E., and Kim, S.: Spatially and chemically resolved source  
868 apportionment analysis: Case study of high particulate matter event, *Atmospheric Environment*,  
869 162, 55-70, <https://doi.org/10.1016/j.atmosenv.2017.05.006>, 2017a.

870 Kim, H. C., Kim, E., Bae, C., Cho, J. H., Kim, B. U., and Kim, S.: Regional contributions to  
871 particulate matter concentration in the Seoul metropolitan area, South Korea: seasonal variation  
872 and sensitivity to meteorology and emissions inventory, *Atmos. Chem. Phys.*, 17, 10315-10332,  
873 10.5194/acp-17-10315-2017, 2017b.



874 Kim, H. C., Kim, S., Kim, B.-U., Jin, C.-S., Hong, S., Park, R., Son, S.-W., Bae, C., Bae, M.,  
 875 Song, C.-K., and Stein, A.: Recent increase of surface particulate matter concentrations in the  
 876 Seoul Metropolitan Area, Korea, Scientific Reports, 7, 4710, 10.1038/s41598-017-05092-8,  
 877 2017c.

878 L., W. P., and Heo, G.: Development of revised SAPRC aromatics mechanism, available at:  
 879 <https://www.engr.ucr.edu/~carter/SAPRC/saprc11.pdf> 2012.

880 Lee, D., Lee, Y.-M., Jang, K.-W., Yoo, C., Kang, K.-H., Lee, J.-H., Jung, S.-W., Park, J.-M.,  
 881 Lee, S.-B., Han, J.-S., Hong, J.-H., and Lee, S.-J.: Korean National Emissions Inventory System  
 882 and 2007 Air Pollutant Emissions, Asian Journal of Atmospheric Environment, 5-4, 278-291,  
 883 2011a.

884 Lee, D.-G., Lee, Y.-M., Jang, K.-W., Yoo, C., Kang, K.-H., Lee, J.-H., Jung, S.-W., Park, J.-M.,  
 885 Lee, S.-B., Han, J.-S., Hong, J.-H., and Lee, S.-J.: Korean National Emissions Inventory System  
 886 and 2007 Air Pollutant Emissions, Asian Journal of Atmospheric Environment, 5,  
 887 10.5572/ajae.2011.5.4.278, 2011b.

888 Lejri, D., Can, A., Schiper, N., and Leclercq, L.: Accounting for traffic speed dynamics when  
 889 calculating COPERT and PHEM pollutant emissions at the urban scale, Transportation Research  
 890 Part D: Transport and Environment, 63, 588-603, <https://doi.org/10.1016/j.trd.2018.06.023>,  
 891 2018.

892 Li, F., Zhuang, J., Cheng, X., Li, M., Wang, J., and Yan, Z.: Investigation and Prediction of  
 893 Heavy-Duty Diesel Passenger Bus Emissions in Hainan Using a COPERT Model, Atmosphere,  
 894 10, 106, 10.3390/atmos10030106, 2019.

895 Li, Q., Qiao, F., and yu, L.: Vehicle Emission Implications of Drivers Smart Advisory System  
 896 for Traffic Operations in Work Zones, Journal of the Air & Waste Management Association, 11,  
 897 10.1080/10962247.2016.1140095, 2016.

898 Liu, H., Guensler, R., Lu, H., Xu, Y., Xu, X., and Rodgers, M.: MOVES-Matrix for High-  
 899 Performance On-Road Energy and Running Emission Rate Modeling Applications, Journal of  
 900 the Air & Waste Management Association, 69, 10.1080/10962247.2019.1640806, 2019.

901 Liu, Y., and Sander, S. P.: Rate Constant for the OH + CO Reaction at Low Temperatures, The  
 902 Journal of Physical Chemistry A, 119, 10060-10066, 10.1021/acs.jpca.5b07220, 2015.

903 Luo, H., Astitha, M., Hogrefe, C., Mathur, R., and Rao, S. T.: A new method for assessing the  
 904 efficacy of emission control strategies, *Atmospheric Environment*, 199, 233-243,  
 905 <https://doi.org/10.1016/j.atmosenv.2018.11.010>, 2019.

906 Lv, W., Hu, Y., Li, E., Liu, H., Pan, H., Ji, S., Hayat, T., Alsaedi, A., and Ahmad, B.: Evaluation  
 907 of vehicle emission in Yunnan province from 2003 to 2015, *J. Clean Prod.*, 207, 814-825,  
 908 <https://doi.org/10.1016/j.jclepro.2018.09.227>, 2019.

909 Moussiopoulos, N., Vlachokostas, C., Tsilingiridis, G., Douros, I., Hourdakakis, E., Naneris, C.,  
 910 and Sidiropoulos, C.: Air quality status in Greater Thessaloniki Area and the emission reductions  
 911 needed for attaining the EU air quality legislation, *Sci. Total Environ.*, 407, 1268-1285,  
 912 <https://doi.org/10.1016/j.scitotenv.2008.10.034>, 2009.

913 Nagpure, A. S., Gurjar, B. R., Kumar, V., and Kumar, P.: Estimation of exhaust and non-exhaust  
 914 gaseous, particulate matter and air toxics emissions from on-road vehicles in Delhi, *Atmospheric  
 915 Environment*, 127, 118-124, [10.1016/j.atmosenv.2015.12.026](https://doi.org/10.1016/j.atmosenv.2015.12.026), 2016.

916 NIER: Study on Air Pollutant Emission Estimation Method in Transportation section(II) 11-  
 917 1480523-003573-01, National Archives of Korea, available at:  
 918 [https://www.archives.go.kr/next/manager/publishmentSubscriptionDetail.do?prt\\_seq=114054&p](https://www.archives.go.kr/next/manager/publishmentSubscriptionDetail.do?prt_seq=114054&p)  
 919 [age=1554&prt\\_arc\\_title=&prt\\_pub\\_kikwan=&prt\\_no](https://www.archives.go.kr/next/manager/publishmentSubscriptionDetail.do?prt_seq=114054&p_age=1554&prt_arc_title=&prt_pub_kikwan=&prt_no) 2018.

920 Ntziachristos, L., and Samaras, Z.: Speed-dependent representative emission factors for catalyst  
 921 passenger cars and influencing parameters, *Atmospheric Environment*, 34, 4611-4619,  
 922 [https://doi.org/10.1016/S1352-2310\(00\)00180-1](https://doi.org/10.1016/S1352-2310(00)00180-1), 2000.

923 Ntziachristos, L., Gkatzoflias, D., Kouridis, C., and Samaras, Z.: COPERT: A European road  
 924 transport emission inventory model, 491-504 pp., 2009.

925 Pedruzzi, R., Baek, B. H., and Wang, C.-T., CARS: <https://github.com/CMASCenter/CARS>,  
 926 last access: MAY, 1st, 2020.

927 Perugu, H., Ramirez, L., and DaMassa, J.: Incorporating temperature effects in California's on-  
 928 road emission gridding process for air quality model inputs, *Environ Pollut*, 239, 1-12,  
 929 [10.1016/j.envpol.2018.03.094](https://doi.org/10.1016/j.envpol.2018.03.094), 2018.

- 930 Perugu, H.: Emission modelling of light-duty vehicles in India using the revamped VSP-based  
 931 MOVES model: The case study of Hyderabad, Transportation Research Part D: Transport and  
 932 Environment, 68, 150-163, <https://doi.org/10.1016/j.trd.2018.01.031>, 2019.
- 933 Pfister, G., Wang, C.-t., Barth, M., Flocke, F., Vizuete, W., and Walters, S.: Chemical  
 934 Characteristics and Ozone Production in the Northern Colorado Front Range, JGR, 2019.
- 935 Pinto, J. A., Kumar, P., Alonso, M. F., Andreão, W. L., Pedruzzi, R., dos Santos, F. S., Moreira,  
 936 D. M., and Albuquerque, T. T. d. A.: Traffic data in air quality modeling: A review of key  
 937 variables, improvements in results, open problems and challenges in current research,  
 938 Atmospheric Pollution Research, 11, 454-468, <https://doi.org/10.1016/j.apr.2019.11.018>, 2020.
- 939 Rao, S. T., Galmarini, S., and Puckett, K.: Air Quality Model Evaluation International Initiative  
 940 (AQMEII): Advancing the State of the Science in Regional Photochemical Modeling and Its  
 941 Applications, Bulletin of the American Meteorological Society, 92, 23-30,  
 942 10.1175/2010BAMS3069.1, 2011.
- 943 Rodríguez-Rey et al. (2021): Rodríguez-Rey, D., Guevara, M., Linares, MP., Casanovas, J.,  
 944 Salmerón, J., Soret, A., Jorba, O., Tena, C., Pérez García-Pando, C.: A coupled macroscopic  
 945 traffic and pollutant emission modelling system for Barcelona, Transportation Research Part D,  
 946 92, <https://doi.org/10.1016/j.trd.2021.102725>, 2021.
- 947 Rinke, M., and Zetzsch, C.: Rate Constants for the Reactions of OH Radicals with Aromatics:  
 948 Benzene, Phenol, Aniline, and 1,2,4-Trichlorobenzene, Berichte der Bunsengesellschaft für  
 949 physikalische Chemie, 88, 55-62, 10.1002/bbpc.19840880114, 1984.
- 950 Russell, A., and Dennis, R.: NARSTO critical review of photochemical models and modeling,  
 951 Atmospheric Environment, 34, 2283-2324, [https://doi.org/10.1016/S1352-2310\(99\)00468-9](https://doi.org/10.1016/S1352-2310(99)00468-9),  
 952 2000.
- 953 Ryu, J. H., Han, J. S., Lim, C. S., Eom, M. D., Hwang, J. W., Yu, S. H., Lee, T. W., Yu, Y. S.,  
 954 and Kim, G. H.: The Study on the Estimation of Air Pollutants from Auto- mobiles (I) -  
 955 Emission Factor of Air Pollutants from Middle and Full sized Buses., in, Transportation  
 956 Pollution Research Center, National Institute of Environmental Research, Incheon, Korea., 2003.
- 957 Ryu, J. H., Lim, C. S., Yu, Y. S., Han, J. S., Kim, S. M., Hwang, J. W., Eom, M. D., Kim, G. Y.,  
 958 Jeon, M. S., Kim, Y. H., Lee, J. T., and Lim, Y. S.: The Study on the Esti- mation of Air  
 959 Pollutants from Automobiles (II) - Emis- sion Factor of Air Pollutants from Diesel Truck., in,

960 Trans- portation Pollution Research Center, National Institute of Environmental Research,  
961 Incheon, Korea., 2004.

962 Ryu, J. H., Yu, Y. S., Lim, C. S., Kim, S. M., Kim, J. C., Gwon, S. I., Jeong, S. W., and Kim, D.  
963 W.: The Study on the Estimation of Air Pollutants from Automobiles (III) - Emission Factor of  
964 Air Pollutants from Small sized Light-duty Vehicles., in, Transportation Pollution Research  
965 Center, National Institute of Environmental Research, Korea., 2005.

966 Sallis, P., Bull, F., Burdett, P., Frank, P., Griffiths, P., Giles-Corti, P., and Stevenson, M.: Use of  
967 science to guide city planning policy and practice: How to achieve healthy and sustainable future  
968 cities, *The Lancet*, 388, 10.1016/S0140-6736(16)30068-X, 2016.

969 Smit, R., Kingston, P., Neale, D. W., Brown, M. K., Verran, B., and Nolan, T.: Monitoring on-  
970 road air quality and measuring vehicle emissions with remote sensing in an urban area,  
971 *Atmospheric Environment*, 218, 116978, <https://doi.org/10.1016/j.atmosenv.2019.116978>, 2019.

972 Sun, W., Duan, N., Yao, R., Huang, J., and Hu, F.: Intelligent in-vehicle air quality  
973 management : a smart mobility application dealing with air pollution in the traffic, 2016.

974 Tominaga, Y., and Stathopoulos, T.: Ten questions concerning modeling of near-field pollutant  
975 dispersion in the built environment, *Build. Environ.*, 105, 390-402,  
976 <https://doi.org/10.1016/j.buildenv.2016.06.027>, 2016.

977 USEPA: Population and Activity of Onroad Vehicles in MOVES3, in, edited by: USEPA, 2020.

978 WHO, Ambient air pollution- a major threat to health and climate:  
979 <https://www.who.int/airpollution/ambient/en/>, last 2019.

980 Xu, X., Liu, H., Anderson, J. M., Xu, Y., Hunter, M. P., Rodgers, M. O., and Guensler, R. L.:  
981 Estimating Project-Level Vehicle Emissions with Vissim and MOVES-Matrix, *Transportation*  
982 *Research Record*, 2570, 107-117, 10.3141/2570-12, 2016.

983 Yarwood, G., and Jung, J.: UPDATES TO THE CARBON BOND MECHANISM FOR  
984 VERSION 6 (CB6), 2010.  
985

## Tables

**Table 1.** Computational processing time by CARS module based on the modeling setup: Total number of activity data = 24,383,578; Emission Factors = 84,608; GIS road links=385,795; districts/states=5,150/16; 9km×9km grid cells=5,494 (82 columns× 67 columns).

No	Module	Desktop i7 (minutes)	Laptop i9 (minutes)	Averaged Time (minutes)
1	<b>Process activity data</b>	1.8	1.5	1.7
2	<b>process emission factors</b>	1.1	0.8	1.0
3	<b>Process shape file</b>	9.9	7.3	8.6
4	<b>Calculate district emissions</b>	6.4	5.7	6.1
5	<b>Grid4AQM [31days]</b>	4.8 [75.9]	5.0 [87.2]	4.9 [81.6]
6	<b>Plot figures</b>	6.2	5.4	5.8
Total [31days]		30.2 [101.3]	25.7 [107.9]	28.1[104.8]

993 **Table 2.** The total emissions comparison between CARS and CAPSS for the 2015 emission.

Emission Inventory	Pollutants (t yr <sup>-1</sup> )					
	NO <sub>x</sub>	VOC	PM2.5	CO	SO <sub>x</sub>	NH <sub>3</sub>
CARS 2015	<b>301,794</b>	<b>61,186</b>	<b>10,108</b>	<b>373,864</b>	<b>172</b>	<b>12,453</b>
CAPSS 2015	369,585	46,145	8,817	245,516	209	10,079

994

995



**Table 3.** The summary tables of emissions (t yr<sup>-1</sup>), contributions (%), and impact factor (IF, kg yr<sup>-1</sup>) per vehicle for criteria air pollutants (CAPs) by vehicle and fuel types: (a) for NO<sub>x</sub>; (b) VOC; (c) for PM<sub>2.5</sub>; (d) for CO; (e) for SO<sub>x</sub>; and (f) for NH<sub>3</sub>.

(a) NO<sub>x</sub>

Vehicle	Gasoline		Diesel		LPG		CNG		Hybrid		Total	
	Emission	IF	Emission	IF	Emission	IF	Emission	IF	Emission	IF	Emission	IF
Sedan	20,219 (6.70%)	1.94	14,783 (4.90%)	12.8	8,159 (2.77%)	4.49	12 (0.00%)	1.26	65 (0.02%)	0.39	43,239 (14.3%)	3.19
Truck	23 (0.01%)	5.54	<b>148,246 (49.1%)</b>	47.9	920 (0.31%)	4.55	88 (0.03%)	66.4	-	-	<b>149,277 (49.5%)</b>	45.2
Bus	0 (0.00%)	0.97	25,677 (8.51%)	<b>340</b>	-	-	9,260 (3.07%)	248	0 (0.00%)	1.77	34,938 (11.6%)	<b>333</b>
SUV	159 (0.05%)	1.19	39,565 (13.1%)	11.4	175 (0.06%)	8.54	0 (0.00%)	1.60	1 (0.00%)	0.42	39,900 (13.2%)	11.0
Van	14 (0.00%)	4.78	16,659 (5.52%)	22.6	1,337 (0.44%)	6.80	0 (0.00%)	1.25	0 (0.00)	0.37	18,012 (6.00%)	19.2
Taxi	-	-	-	-	1,217 (0.40%)	2.11	-	-	-	-	1,217 (0.40%)	2.11
Special	1 (0.00%)	20.1	12,347 (4.10%)	152	0 (0.00%)	0.52	-	-	-	-	12,375 (4.10%)	151
Motorcycle	2,836 (0.94%)	1.31	-	-	-	-	-	-	-	-	2,836 (0.94%)	1.32
Total	23,253 (7.70%)	1.83	<b>257,305 (85.3%)</b>	29.9	11,809 (3.91%)	4.20	9,361 (3.10%)	<b>36.7</b>	66 (0.02%)	0.39	301,794 (100%)	13.3

(b) VOC

Vehicle	Gasoline		Diesel		LPG		CNG		Hybrid		Total	
	Emission	IF	Emission	IF	Emission	IF	Emission	IF	Emission	IF	Emission	IF
Sedan	28,434 (46.5%)	2.73	629 (1.03%)	0.55	2,107 (3.44%)	1.16	3 (0.01%)	0.33	77 (0.13%)	0.47	<b>31,250 (51.1%)</b>	2.30
Truck	23 (0.04%)	5.44	8,194 (13.4%)	2.65	286 (0.47%)	1.41	102 (0.17%)	77.2	-	-	8,605 (14.1%)	2.61
Bus	0 (0.00%)	1.65	717 (1.17%)	9.51	-	-	11,942 (19.5%)	320	0 (0.00%)	0	12,659 (20.7%)	<b>112</b>
SUV	246 (0.40%)	1.84	2,441 (3.99%)	0.71	46 (0.08%)	2.25	0 (0.00%)	0.75	1 (0.00%)	0.55	2,733 (4.47%)	0.76
Van	21 (0.03%)	7.04	1,185 (1.94%)	1.61	393 (0.64%)	2.00	0 (0.00%)	0.45	0 (0.00%)	0	1,599 (2.61%)	1.71
Taxi	-	-	-	-	273 (0.45%)	0.47	-	-	-	-	273 (0.45%)	0.47
Special	1 (0.00%)	25.8	904 (1.48%)	11.1	0 (0.00%)	0.23	-	-	-	-	905 (1.48%)	11.0
Motorcycle	3,160 (5.16%)	1.46	-	-	-	-	-	-	-	-	3,160 (5.16%)	1.46
Total	<b>31,885 (52.1%)</b>	2.50	14,070 (23.0%)	1.64	3,106 (5.08%)	1.10	12,047 (19.7%)	<b>247</b>	78 (0.13%)	0.47	61,186 (100%)	2.51

(c) PM<sub>2.5</sub>

Vehicle	Gasoline		Diesel		LPG		CNG		Hybrid		Total	
	Emission	IF	Emission	IF	Emission	IF	Emission	IF	Emission	IF	Emission	IF
Sedan	144 (1.42%)	0.01	809 (8.00%)	0.70	0	0	0	0	3 (0.03%)	0.02	956 (9.46%)	0.07
Truck	0 (0.01%)	0	<b>5,415 (53.6%)</b>	1.75	0	0	0	0	-	-	<b>5,415 (53.6%)</b>	1.64
Bus	0	0	214 (2.11%)	<b>2.83</b>	-	-	0	0	0 (0.01%)	0.09	214 (2.11%)	1.89
SUV	2 (0.02%)	0.02	2,165 (21.4%)	0.63	0	0	0	0	0	0.02	2,167 (21.4%)	0.60
Van	0	0	1,127 (11.2%)	1.53	0	0	0	0	0	0.02	1,127 (11.2%)	1.20
Taxi	-	-	-	-	0	0	-	-	-	-	0	0
Special	0	0	230 (2.28%)	2.82	0	0	-	-	-	-	230 (2.28%)	<b>2.81</b>
Motorcycle	0	0	-	-	-	-	-	-	-	-	0	0
Total	146 (1.44%)	0.01	<b>9,959 (98.5%)</b>	<b>1.16</b>	0	0	0	0	3 (0.03%)	0.02	10,108 (100%)	0.41

1007  
1008 (d) CO

Vehicle	Gasoline		Diesel		LPG		CNG		Hybrid		Total	
	Emission	IF	Emission	IF	Emission	IF	Emission	IF	Emission	IF	Emission	IF
Sedan	178,121 (47.6%)	17.1	3,436 (0.92%)	2.98	42,886 (11.5%)	23.6	29 (0.01%)	2.91	177 (0.05%)	1.07	<b>224,649 (60.1%)</b>	16.6
Truck	254 (0.07%)	61.1	47,065 (12.6%)	15.2	9,088 (2.43%)	44.9	68 (0.02%)	51.4	-	-	56,475 (15.1%)	17.1
Bus	0 (0.00%)	19.3	7,633 (2.05%)	<b>101</b>	-	-	1542 (0.41%)	41.3	1 (0.00%)	4.64	9,176 (2.45%)	<b>81.2</b>
SUV	2,616 (0.70%)	19.6	13,401 (3.58%)	3.87	791 (0.21%)	38.6	0 (0.00%)	4.09	2 (0.00%)	1.15	16,808 (4.50%)	4.65
Van	131 (0.04%)	43.4	6,611 (1.77%)	8.97	8,032 (2.15%)	40.9	2 (0.00%)	6.53	0 (0.00%)	1.00	14,777 (3.95%)	15.8
Taxi	-	-	-	-	8,481 (2.27%)	14.7	-	-	-	-	8,481 (2.27%)	14.7
Special	13 (0.00%)	269	4,224 (1.13%)	51.7	1 (0.00%)	3.69	-	-	-	-	4,239 (1.13%)	51.7
Motorcycle	39,256 (10.5%)	18.2	-	-	-	-	-	-	-	-	39,256 (10.5%)	18.2
Total	<b>220,390 (59.0%)</b>	17.3	82,372 (22.0%)	9.57	69,281 (18.5%)	<b>24.6</b>	1641 (0.44%)	33.6	180 (0.05%)	1.07	373,864 (100%)	15.4

1009  
1010 (e) SO<sub>x</sub>

Vehicle	Gasoline		Diesel		LPG		CNG		Hybrid		Total	
	Emission	IF	Emission	IF	Emission	IF	Emission	IF	Emission	IF	Emission	IF
Sedan	51.3 (29.8%)	0.005	6.5 (3.79%)	0.006	8.28 (4.81%)	0.005	0	0	1.14 (0.67%)	0.007	<b>67.2 (39.1%)</b>	0.005
Truck	0.03 (0.02%)	0.008	45.5 (26.5%)	0.015	0.97 (0.57%)	0.005	0	0	-	-	46.5 (27.1%)	0.014
Bus	0 (0.00%)	0.003	10.8 (6.26%)	<b>0.143</b>	-	-	0	0	0.01 (0.01%)	0.047	10.8 (6.26%)	<b>0.095</b>
SUV	0 (0.00%)	0.000	18.2 (10.6%)	0.005	0.00 (0.00%)	0.000	0	0	0.01 (0.01%)	0.007	18.2 (10.6%)	0.005
Van	0.02 (0.01%)	0.006	5.5 (3.20%)	0.007	0.77 (0.45%)	0.004	0	0	0 (0.00%)	0.010	6.30 (3.66%)	0.007
Taxi	-	-	-	-	7.71 (4.49%)	0.013	-	-	-	-	7.71 (4.48%)	0.013
Special	0 (0.00%)	0.003	7.3 (4.27%)	0.090	0.00 (0.00%)	0.005	-	-	-	-	7.34 (4.27%)	0.090
Motorcycle	7.94 (4.62%)	0.004	-	-	-	-	-	-	-	-	7.94 (4.62%)	0.004
Total	59.3 (34.5%)	0.006	<b>93.8 (54.5%)</b>	<b>0.011</b>	17.7 (10.3%)	0.006	0	0	1.17 (0.68%)	0.007	172 (100%)	0.007

1011  
1012  
1013 (e) NH<sub>3</sub>

Vehicle	Gasoline		Diesel		LPG		CNG		Hybrid		Total	
	Emission	IF	Emission	IF	Emission	IF	Emission	IF	Emission	IF	Emission	IF
Sedan	12,225 (98.3%)	<b>1.17</b>	20 (0.16%)	0.02	0	0.00	0	0	19 (0.15%)	0.11	<b>12,284 (98.6%)</b>	<b>0.91</b>
Truck	0 (0.00%)	0.03	82 (0.66%)	0.03	0	0.00	0	0	-	-	82 (0.66%)	0.02
Bus	0 (0.00%)	0.09	15 (0.12%)	0.19	-	-	0	0	0 (0.00%)	0.51	15 (0.12%)	0.13
SUV	0 (0.00%)	0.00	0 (0.00%)	0.00	0	0.00	0	0	0 (0.00%)	0.16	0 (0.00%)	0.00
Van	0 (0.00%)	0.02	14 (0.11%)	0.02	0	0.00	0	0	0 (0.00%)	0.09	14 (0.11%)	0.01
Taxi	-	-	-	-	0	0.00	-	-	-	-	0 (0.00%)	0.00
Special	0 (0.00%)	0.01	10 (0.08%)	0.12	0	0.00	-	-	-	-	10 (0.08%)	0.12
Motorcycle	49 (0.39%)	0.02	-	-	-	-	-	-	-	-	49 (0.39%)	0.02
Total	<b>12,293 (98.7%)</b>	<b>0.97</b>	141 (1.13%)	0.02	0	0.00	0	0	19 (0.16%)	0.12	12,453 (100%)	0.51

1014  
1015

Figures

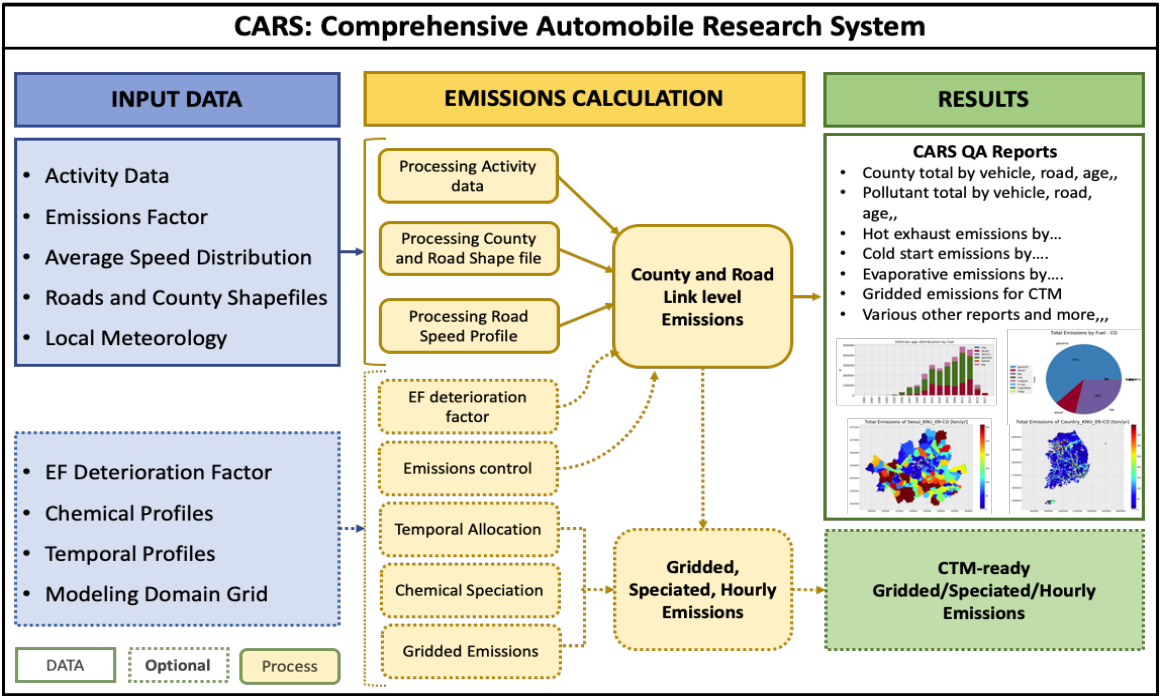


**Figure 1.** CARS schematic methodology to estimate mobile emissions.

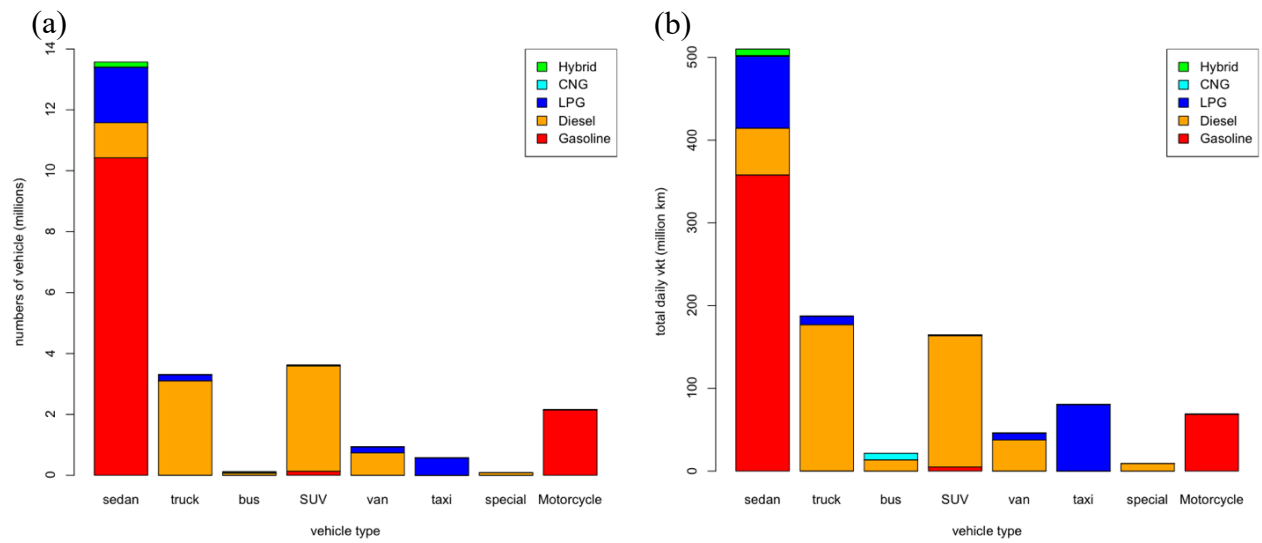


**Figure 2. (a)** The number of vehicles by vehicle and fuel types and **(b)** the total daily VKT by vehicle and fuel types in South Korea.

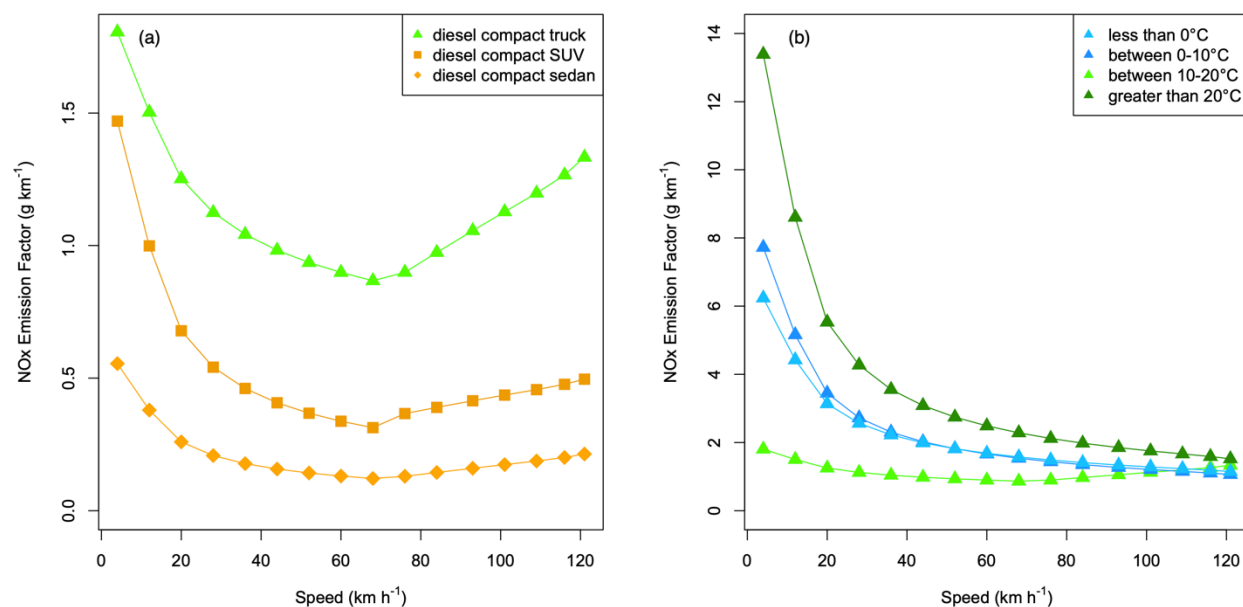


**Figure 3.** Variation of NO<sub>x</sub> emission factors from diesel compact engines by vehicle speed and ambient temperatures: **(a)** NO<sub>x</sub> emission factors function to vehicle speed; **(b)** NO<sub>x</sub> emission factors of diesel compact truck function to vehicle speed and ambient temperature.

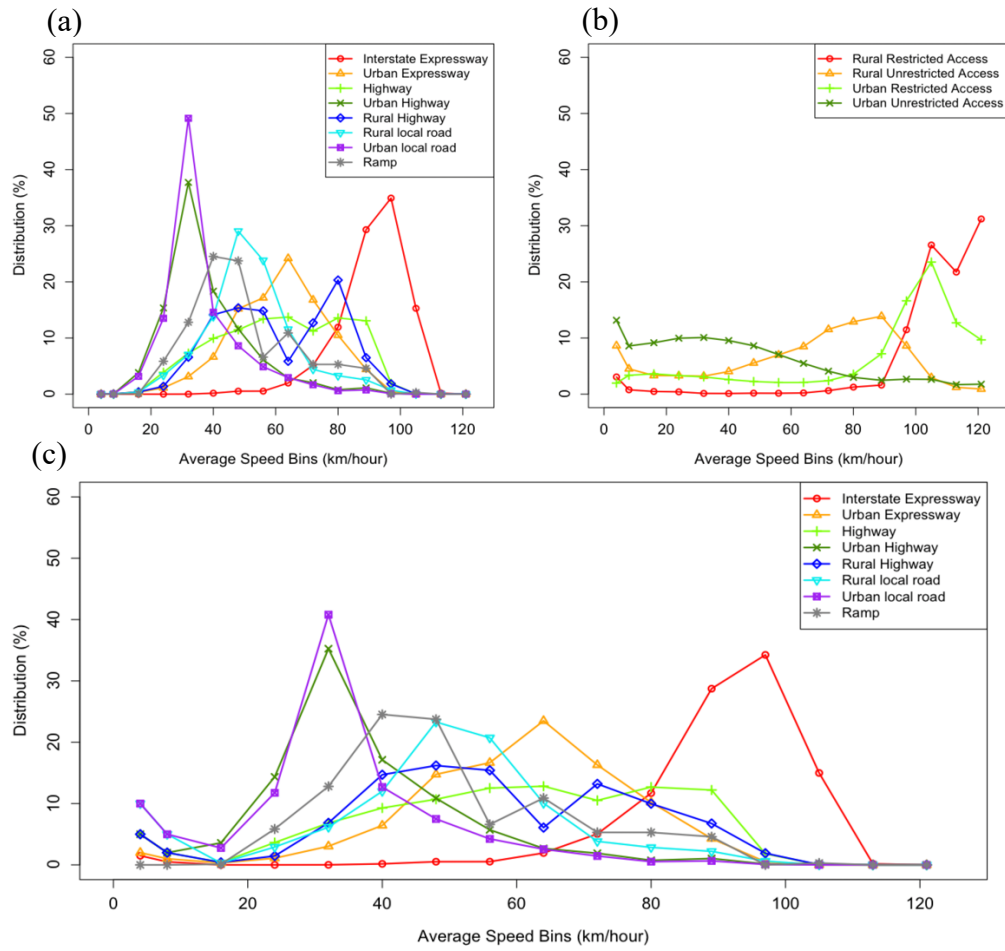


**Figure 4.** (a) The South Korea speed distribution by road types. (b) The Georgia state speed distribution by road types. (c) The average speed distribution (ASD) by road types used in this study for South Korea.

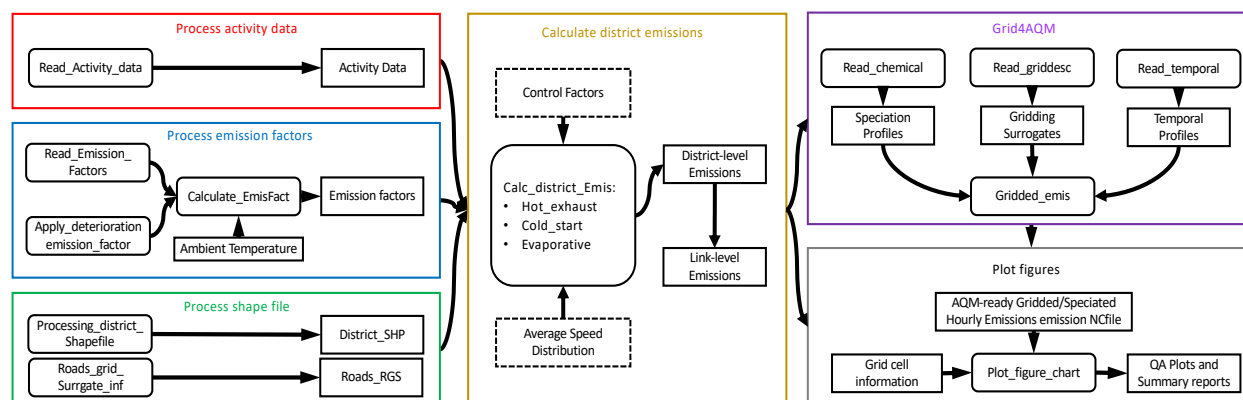


**Figure 5.** The schematic of modules and their functions in the CARS.

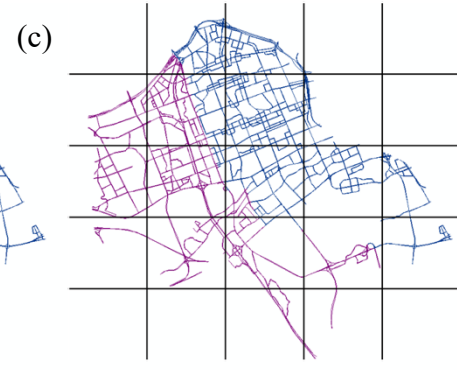
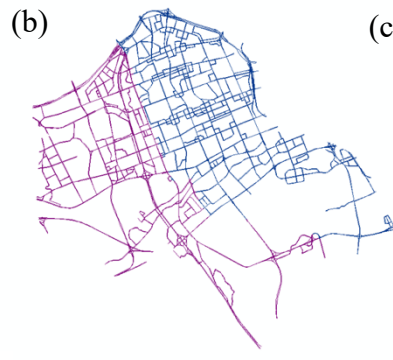


**Figure 6** (a) the road network GIS shapefile of Seoul, South Korea; (b) two districts with different colors (purple and blue); (c) the modeling grid cells over road segments.



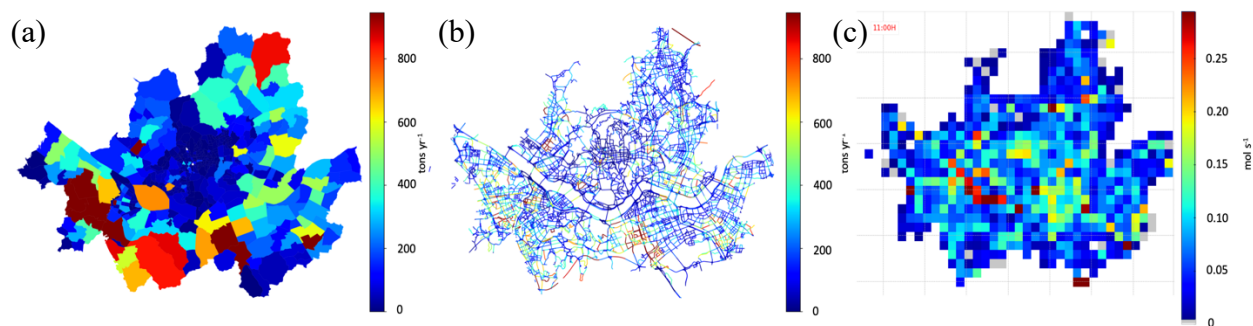


**Figure 7.** Three different formats of CO emissions from CARS, (A) District-level total emissions ( $\text{t yr}^{-1}$ ) (B) Link-level total emissions ( $\text{t yr}^{-1}$ ), (C) CTM-ready gridded hourly total emissions ( $\text{moles s}^{-1}$ ).

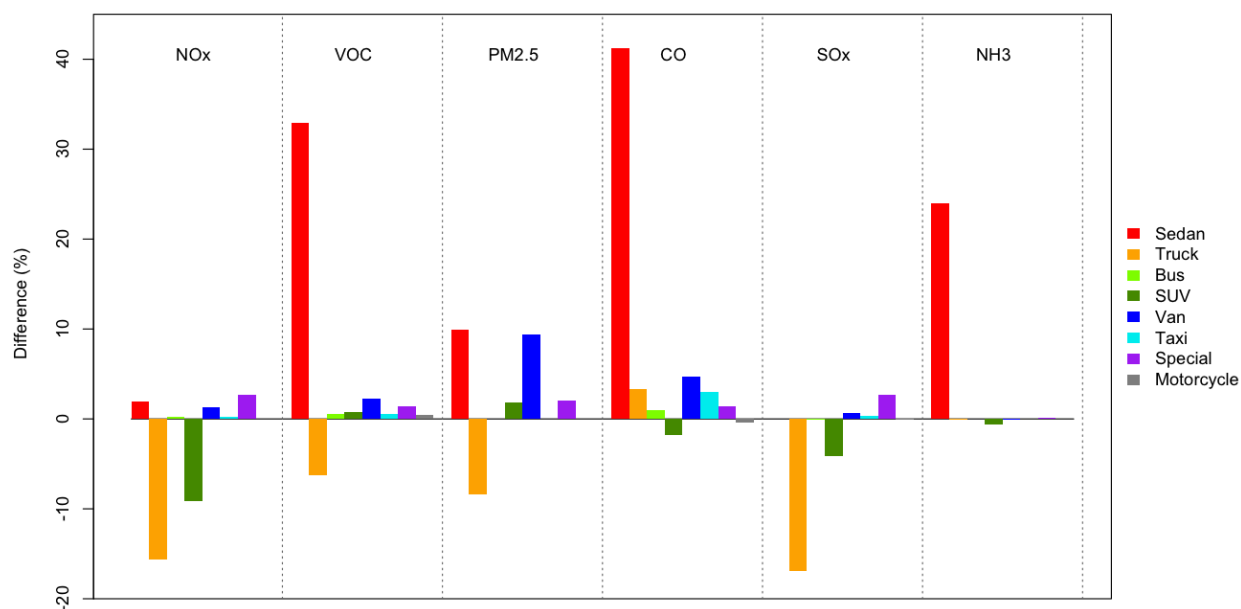


**Figure 8.** Comparison between CARS 2015 and CAPSS 2015 onroad mobile emissions inventories by vehicle types. The standard line is CAPSS 2015 data.

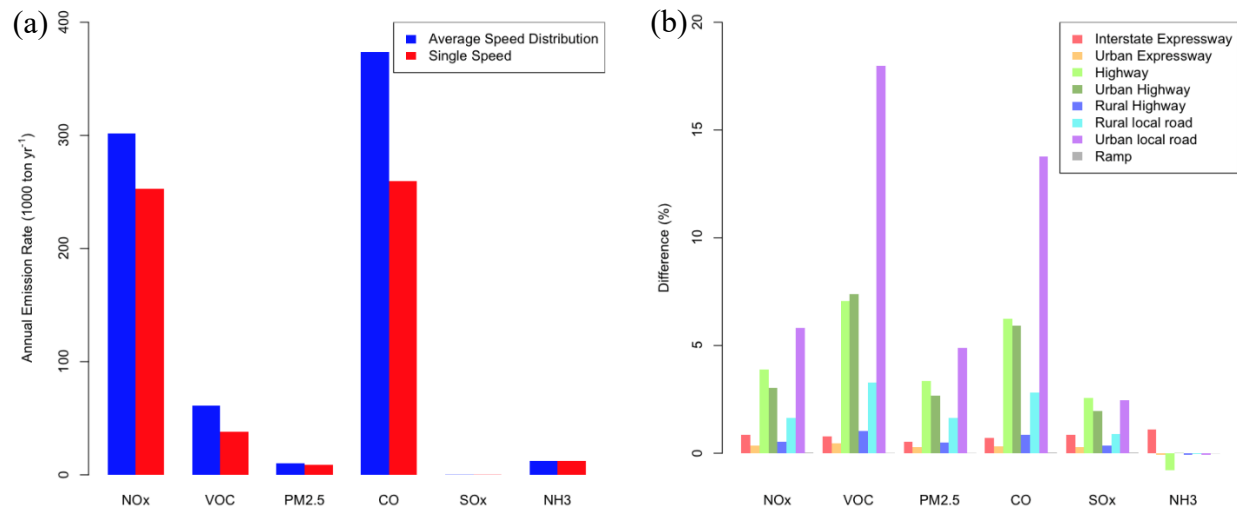


**Figure 9.** The impacts of emissions between the ASD and single-speed approach: (a) the total emission differences by pollutant; (b) The road-specific difference (%) by pollutant.

## Appendix

**Appendix A:** The vehicle types classified by fuel type, vehicle body type, and engine size. The emission factors of the diesel vehicle with the star (\*) are depended on the ambient temperature (*T*).

Vehicle Types	Fuel Types							
	Gasoline	Diesel	LPG	CNG	HYBRID G	HYBRID D	HYBRID L	HYBRID C
Sedan	Supercompact	Supercompact*	Supercompact	-	-	-	-	-
	Compact	compact*	compact	compact	compact	compact	compact	-
	Fullsize	Fullsize*	Fullsize	Fullsize	Fullsize	Fullsize	Fullsize	-
	Midsize	Midsize*	Midsize	Midsize	Midsize	Midsize	Midsize	-
Truck	Supercompact	Supercompact	Supercompact	-	-	-	-	-
	Compact	Compact*	Compact	Compact	-	-	-	-
	Fullsize	Concrete	-	Fullsize	-	-	-	-
	Midsize	Fullsize	Midsize	Midsize	-	-	-	-
	-	Midsize	-	-	-	-	-	-
	-	Dump	-	-	-	-	-	-
Bus	Urban	Urban	Urban	Urban	-	Urban	-	-
	-	Rural	-	Rural	-	Rural	-	Rural
SUV	Compact	Compact*	Compact	-	-	-	-	-
	Midsize	Midsize*	Midsize	Midsize	Midsize	-	-	-
Van	supercompact	supercompact	supercompact	-	-	-	-	-
	Compact	Compact	Compact	Compact	-	-	-	-
	-	-	Fullsize	Fullsize	Fullsize	Fullsize	Fullsize	Fullsize
Taxi	Midsize	Midsize	Midsize	Midsize	Midsize	Midsize	Midsize	Midsize
	-	-	Compact	-	-	-	-	-
	-	-	Fullsize	-	-	-	-	-
Special	-	-	Midsize	-	-	-	-	-
	-	Tow	-	-	-	-	-	-
	Wrecking	Wrecking	Wrecking	Wrecking	-	-	-	-
Motorcycle	Others	Others	Others	-	-	-	-	-
	Compact	-	-	-	-	-	-	-
	Midsize	-	-	-	-	-	-	-
	Fullsize	-	-	-	-	-	-	-

- no existence

\* ambient temperature-dependent diesel vehicle

LPG: Liquefied Petroleum Gas

CNG: Connecticut Natural Gas

Hybrid\_G: hybrid vehicle with gasoline

Hybrid\_D: hybrid vehicle with diesel

Hybrid\_L: hybrid vehicle with LPG

Hybrid\_C: hybrid vehicle with CNG

1074 **Appendix B**, The summary of activity data (number of vehicles and daily total VKTs) in South  
1075 Korea by vehicle type with engine size.

Vehicle Types	Engine sizes	Fuel Types									
		Gasoline		Diesel		LPG		CNG		Hybrid	
		Numbers	Daily VKT	Numbers	Daily VKT	Numbers	Daily VKT	Numbers	Daily VKT	Numbers	Daily VKT
Sedan	Supercompact	1,792,471	50,197,345	46	1,761	83,226	4,000,067	6	237	-	-
	Compact	1,372,317	39,543,668	51,324	2,570,086	8,040	257,060	276	12,115	3,802	137,360
	Fullsize	2,403,327	100,632,702	428,831	20,928,552	292,850	15,910,588	5,296	323,852	21,533	1,086,509
	Midsized	4,858,533	167,454,032	672,960	33,126,318	1,431,970	66,640,378	4,310	625,717	140,527	6,717,856
Truck	Supercompact	850	9,595	816	354	111,051	6,550,476	-	-	-	-
	Compact	3,185	143,510	2,655,089	133,480,216	87,650	3,567,109	42	2,694	-	-
	Fullsize	3	422	180,991	25,774,819	-	-	72	4,676	-	-
	Midsized	98	7,430	258,509	17,477,685	1,434	47,870	14	483	-	-
	Dump	-	-	-	-	-	-	-	-	-	-
	Special	20	970	-	-	2,292	99,124	1,194	60,886	-	-
Bus	Urban	1	126	40,448	7,282,593	1	652	6,543	1,466,854	2	282
	Rural	-	-	34,997	6,334,278	-	-	30,792	6,460,001	216	50,873
SUV	Compact	42,348	1,395,153	2,341,397	105,962,626	6,946	275,728	13	551	-	-
	Midsized	91,002	3,520,552	1,120,128	5,277,861	13,567	595,426	15	706	1,719	88,683
Van	supercompact	88	1,645	-	-	44,947	2,058,014	-	-	-	-
	Compact	2,937	87,507	685,317	34,781,937	151,654	6,135,138	7	255	-	-
	Fullsize	-	-	19,452	1,318,221	1	14	97	7,598	3	136
	Midsized	2	1,303,795	31,790	1,433,407	15	416	160	15,216	2	85
	Special	-	-	-	-	-	-	-	-	-	-
Taxi	Compact	-	-	-	-	8,380	576,378	-	-	-	-
	Fullsize	-	-	-	-	92,861	10,827,756	-	-	-	-
	Midsized	-	-	-	-	474,455	69,087,721	-	-	-	-
Special	Tow	-	-	40,807	7,447,773	-	-	-	-	-	-
	Wrecking	2	138	12,568	813,746	128	6,607	3	94	-	-
	Others	47	553	28,275	989,988	180	9,966	-	-	-	-
Motorcycle	Compact	184,822	3,507,948	-	-	-	-	-	-	-	-
	Fullsize	65,964	3,493,728	-	-	-	-	-	-	-	-
	Midsized	1,910,988	61,676,824	-	-	-	-	-	-	-	-

- 1076 - no existence  
1077 LPG: Liquefied Petroleum Gas  
1078 CNG: Connecticut Natural Gas  
1079 Hybrid: all hybrid vehicles, electric power mixed with fossil fuel (gasoline, diesel, LPG, or CNG)  
1080  
1081  
1082

**Appendix C**, Eight road types with assigned average vehicle operating speed and VKT fractions.

Road types	Description	Average Speed (km h <sup>-1</sup> )	Road VKT fraction
101	Interstate Expressway	90	41%
102	Urban Expressway	60	5%
103	Highway	58	18%
104	Urban Highway	36	12%
105	Rural Highway	55	3%
106	Rural Local Road	45	4%
107	Urban Local Road	32	17%
108	Ramp	50	0.4%

**Appendix D**, The daily average VKT (km d<sup>-1</sup>) per vehicle by vehicle and fuel types.

Vehicle types	Fuel Types					
	Gasoline	Diesel	LPG	CNG	Hybrid	Average
Sedan	34	49	48	97	48	38
Truck	39	57	51	52	-	57
Bus	126	180	-	212	237	191
SUV	37	46	42	45	52	46
VAN	29	51	42	87	44	49
Taxi	-	-	140	-	-	140
Special	14	113	54	31	-	113
Motorcycle	32	-	-	-	-	32

1090 **Appendix E**, Average speed distribution (ASD) for each road type: The table columns are  
 1091 different road types, and the table rows are average speed of each speed bin.

Speed bins	Speed (km/h)	Road Types							
		101	102	103	104	105	106	107	108
1	speed < 4	1.50%	2.00%	5.00%	5.00%	5.00%	10.00%	10.00%	0.00%
2	4 ≤ speed < 8	0.50%	1.00%	2.00%	2.00%	2.00%	5.00%	5.00%	0.00%
3	8 ≤ speed < 16	0.00%	0.33%	0.40%	3.59%	0.41%	0.30%	2.76%	0.11%
4	16 ≤ speed < 24	0.00%	1.09%	3.64%	14.35%	1.45%	2.91%	11.75%	5.85%
5	24 ≤ speed < 32	0.01%	3.04%	6.82%	35.25%	6.85%	6.15%	40.80%	12.80%
6	32 ≤ speed < 40	0.17%	6.43%	9.28%	17.14%	14.70%	12.00%	12.69%	24.53%
7	40 ≤ speed < 48	0.52%	14.76%	10.70%	10.86%	16.20%	23.30%	7.49%	23.74%
8	48 ≤ speed < 56	0.53%	16.66%	12.52%	5.72%	15.42%	20.72%	4.24%	6.60%
9	56 ≤ speed < 64	1.94%	23.49%	12.83%	2.68%	6.08%	10.06%	2.56%	10.90%
10	64 ≤ speed < 72	5.05%	16.30%	10.51%	1.90%	13.21%	3.84%	1.45%	5.30%
11	72 ≤ speed < 80	11.70%	10.19%	12.69%	0.74%	9.98%	2.85%	0.53%	5.30%
12	80 ≤ speed < 89	28.73%	4.30%	12.21%	1.04%	6.75%	2.21%	0.65%	4.59%
13	89 ≤ speed < 97	34.24%	0.51%	1.82%	0.15%	1.90%	0.62%	0.08%	0.00%
14	97 ≤ speed < 105	14.99%	0.00%	0.02%	0.00%	0.04%	0.03%	0.00%	0.30%
15	105 ≤ speed < 113	0.18%	0.00%	0.00%	0.00%	0.00%	0.00%	0.00%	0.00%
16	113 ≤ speed < 121	0.01%	0.00%	0.00%	0.00%	0.00%	0.00%	0.00%	0.00%

1092 **Appendix F: Single average speed** for each road type

Speed bins	Speed (km/h)	Road Types							
		101	102	103	104	105	106	107	108
1	speed < 4	0%	0%	0%	0%	0%	0%	0%	0%
2	4 ≤ speed < 8	0%	0%	0%	0%	0%	0%	0%	0%
3	8 ≤ speed < 16	0%	0%	0%	0%	0%	0%	0%	0%
4	16 ≤ speed < 24	0%	0%	0%	0%	0%	0%	0%	0%
5	24 ≤ speed < 32	0%	0%	0%	0%	0%	0%	100%	0%
6	32 ≤ speed < 40	0%	0%	0%	100%	0%	0%	0%	0%
7	40 ≤ speed < 48	0%	0%	0%	0%	0%	100%	0%	100%
8	48 ≤ speed < 56	0%	0%	100%	0%	100%	0%	0%	0%
9	56 ≤ speed < 64	0%	100%	0%	0%	0%	0%	0%	0%
10	64 ≤ speed < 72	0%	0%	0%	0%	0%	0%	0%	0%
11	72 ≤ speed < 80	0%	0%	0%	0%	0%	0%	0%	0%
12	80 ≤ speed < 89	100%	0%	0%	0%	0%	0%	0%	0%
13	89 ≤ speed < 97	0%	0%	0%	0%	0%	0%	0%	0%
14	97 ≤ speed < 105	0%	0%	0%	0%	0%	0%	0%	0%
15	105 ≤ speed < 113	0%	0%	0%	0%	0%	0%	0%	0%
16	113 ≤ speed < 121	0%	0%	0%	0%	0%	0%	0%	0%

1093

## Appendix G:

The annual emission rate between original road type ASD, adjusted road type ASD, and CAPSS result for 2015

Gg/year	CO	NOx	SOx	PM10	PM2.5	VOC	NH3
CARS data 2015 org ASD	269.3	258.4	0.2	9.5	8.8	38.9	12.4
CARS data 2015 adj ASD	373.9	301.8	0.2	11.0	10.1	61.2	12.5
CAPSS 2015	245.5	369.6	0.2	9.6	8.8	46.1	10.1

## Appendix H:

CARS model input data summary table

Input data type	Parameters	Variable Name in CARS	File format
Human activity data of each vehicle	Fuel, vehicle, type, daily VKT, region code, manufacture data	activity_file	csv
Emission factor table	Vehicle, engine, fuel, SCC ,Pollutant, year, temperature, v,a,b,c,d,f,k	Emis_factor_list	csv
Link level Shape file	Link ID, region code, region name, road rank, speed, VKT, Link length, geometry	Link_shape	shape file
County Shape File	Region code, region name	county_shape	shape file
Average speed distribution table	Speed bins, the distribution of each road type	avg_SPD_Dist_file	csv
road restriction table	Vehicle, engine, fuel, road types	road_restriction	csv
Vehicle deterioration table	Vehicle, engine, SCC, fuel, Pollutant, Manufacture date	Deterioration_list	csv
Control strategy factors table	Vehicle, engine, fuel, year, data, region code, control factor	control_list	csv
Model domain description	Projection method name, parameters for prjection method, domain name, bottum left coner X and Y, grid cell size, numbers of grid cell in X, Y, and Z-axis	gridfile_name	text file in griddesc format
Temporal profile tables	Profile reference number, Year to Monthly profile (12 columns)	temporal_monthly_file	csv
	Profile reference number, week to daily profile (7 columns)	temporal_week_file	csv



	Profile reference number, week day to hourly profile (24 columns)	temporal_weekday_file	csv
	Profile reference number, weekend day to hourly profile (24 columns)	temporal_weekend_file	csv
	Vehicle, types, fuel, road type, month reference number, week reference number, weekday reference number, weekend reference number	temporal_CrossRef	csv
<b>Chemical profile table</b>	Species code, species name, target species name, fraction, molecular weight,	Chemical_profile	txt or csv
	Vehicle, engine, fuel, species reference codes	speciation_CrossRef	csv

1104  
1105